I. MILLIMETER MICROWAVE SPECTROSCOPY OF RADICALS

II. LASER SPECTROSCOPY OF THE VAN DER WAALS MOLECULE Ne-Cl_2

Thesis by

David Edward Brinza

In Partial Fulfillment of the Requirements

for the Degree of

Doctor of Philosophy

California Institute of Technology

Pasadena, California

1984

(Submitted September 30, 1983)

For Melinda

and

For My Mother

Acknowledgments

I am deeply indebted to my research advisors, Ken Janda and Herb Pickett, for the guidance they so expertly provided throughout my graduate student career. The level of understanding exhibited by Herb in so many of the technological and theoretical aspects of chemical physics remains for me, truly inspirational. I am especially thankful to Ken for the support, encouragement, and frequent insightful suggestions which helped make my experience at Caltech a rewarding adventure.

My association with the other members of the Janda group has been most enjoyable. Colin Western taught me a great deal about the right way to use computers in the laboratory. Fellow graduate students Mike Casassa, Francis Celii, and Barry Swartz, have been good friends as well as helpful colleagues during the past years. To the new graduate students, Dwight Evard and Sally Hair, go my thanks for the assistance they have rendered.

The cooperation and expertise of the members of the technical staff simplified the design and construction of the apparatus immensely. The stockroom personnel were always helpful and became good friends over the years. I also thank the people of the Fiscal Office for the efficient handling of the numerous requistions that were made.

I owe a great deal to the people who have become my closest friends. Lee has helped make some of the more difficult times a bit less painful. Coach Parker and members of the 1981 and 1982 winning football teams have made those seasons unforgettably enjoyable experiences. Several others, particularly Dan and Gerry, Tony M., and Mike O., were responsible for some of my very best times here.

Finally, I cannot begin to express my graditude towards the most important person in my life, my wife Melinda. She has made sacrifices in her musical career in order to allow me to pursue my own goals. Her love and understanding have helped me through the toughest times. Being able to share the happy moments with her made them even better. I also thank her for assisting in the typing of this thesis.

Abstract

The temperature dependence of the linewidth parameter for the pressure broadening of ClO rotational transitions was investigated. As determined from millimeter microwave spectroscopy, the value of the linewidth parameter at 218K is 4.44±0.23 MHz/torr. The width parameter varies according to $T^{-0.75\pm0.2}$ over the temperature range 200-350K. A similar study was carried out for oxygen self-broadening and broadening by nitrogen. The stronger temperature dependence for the self-broadened case suggests a resonant spin-flip or exchange process is important in the collisional broadening.

The measurement of microwave spectra of the CS radical, as produced in the ArF excimer laser photolysis (193 nm.) of CS_2 was attempted. No spectra for the vibrationally excited CS molecules produced in the photolysis could be observed, presumably due to relatively slow rotational relaxation of the CS fragment.

The van der Waals molecule Ne-Cl_2 has been studied by molecular beam laser spectroscopy. Fluorescence features ~6 cm^{-1} to higher energy of the Cl_2 $B-X$ band origins are attributed to Ne-Cl_2. Band shape analysis supports a T-shaped molecular structure. The metastable vibrationally excited molecule Ne-Cl_2 ($X^1\Sigma^+, v''=1$) has been spectroscopically observed. The time-of-flight from the nozzle indicates the lifetime of the complex to be greater than 10^{-5} sec.

Table of Contents

List of Figures

List of Tables

Chapter I

A. Pressure Broadening of ClO by Nitrogen

B. Pressure Broadening of Oxygen and its Implications for Cosmic Background Measurements

Pressure Broadening of ClO by Nitrogen

H. M. Pickett, D. E. Brinza, and E. A. Cohen

ABSTRACT

The temperature and pressure dependence of linewidths for the $J = 11/2 \leftarrow 9/2$ and $J = 15/2 \leftarrow 13/2$ transitions of ClO have been determined by microwave spectroscopy. The widths for both transitions are found to be the same within experimental error. The width parameter γ for nitrogen broadening is 3.35±0.17 MHz/torr at 317K and 4.44±0.23 MHz/torr at 218K.

I. Introduction

The importance of ClO as a catalytic species in stratospheric ozone depletion is of current interest. A ClO distribution in the upper atmosphere has been modeled by a number of workers (see, for example, Logan *et al.*[1]). Measurement of volume mixing ratios of stratospheric ^{35}ClO is now performed by means of aircraft-based and ground-based microwave emission spectrometers.[2,3] The profiles obtained by analysis of the $J = 9/2 \leftarrow 7/2$, $J = 11/2 \leftarrow 9/2$ and $J = 15/2 \leftarrow 13/2$ transitions at 167 GHz, 241 GHz, and 278 GHz respectively are sensitive to the value of the pressure broadening parameter γ used in the collisional lineshape function. Waters, *et al.*[2] estimated $\gamma = 4.2$ MHz/torr, for ClO ($\mu = 1.24$D) by linear interpolation of values for HF ($\gamma = 4.86$ MHz/torr, $\mu = 1.8$D) and CO ($\gamma = 3.16$ MHz/torr, $\mu = 0.11$D). This paper describes the determination of γ for ClO at 207K and 278K, by N_2 line broadening of the $J = 11/2 \leftarrow 9/2$, and $J = 15/2 \leftarrow 13/2$ transitions of $v=0$ $^2\Pi_{3/2}$ ^{35}ClO.

II. Experimental

The submillimeter source used in these measurements was a frequency stabilized klystron whose output is multiplied by a diode multiplier. Frequency measurements and stabilization was achieved by comparison of the klystron output with some multiple of an X-band (8-12 GHz) oscillator as shown in Figure 1. The X-band source is phase-locked by a commercial phase-lock loop stabilizer and is counted by a frequency counter. A sample of the klystron output and the X-band are fed into a harmonic mixer, and the resulting IF is coupled into a 1120-1220 MHz amplifier. A portion of the IF is sampled and displayed by the spectrum

Figure 1. Block diagram of submillimeter spectrometer.

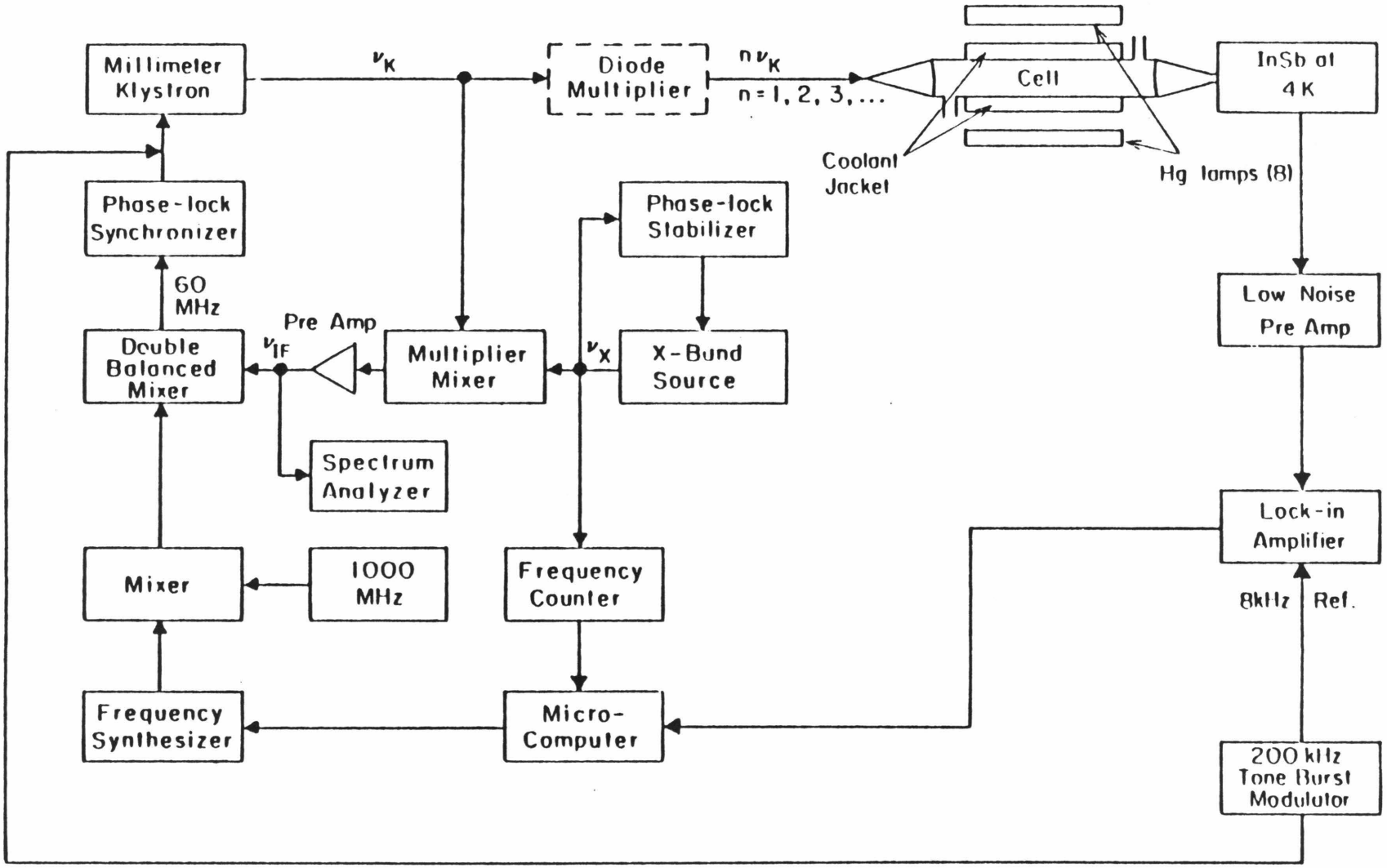
Millimeter Klystron
ν_K
Diode Multiplier
$n\nu_K$
n = 1, 2, 3, ...
Cell
InSb at 4 K
Coolant Jacket
Hg lamps (8)
Phase-lock Synchronizer
Phase-lock Stabilizer
60 MHz
Pre Amp
Low Noise Pre Amp
Double Balanced Mixer
ν_{IF}
Multiplier Mixer
ν_X
X-Band Source
Spectrum Analyzer
Lock-in Amplifier
Mixer
1000 MHz
Frequency Counter
8kHz
Ref.
Frequency Synthesizer
Micro-Computer
200 kHz Tone Burst Modulator

analyzer and the remainder is passed to a double balanced mixer. Here a synthesized frequency of 1060 MHz to 1160 MHz down-converts the IF to produce a 60 MHz signal for the phase-lock synchronizer. The phase-lock synchronizer uses a digital phase-frequency detector described by Pickett[4] which provides a nearly linear phase-voltage output over a range of nearly $\pm 2\pi$.

Microwave power absorption is generally detected by some modulation scheme. In tone-burst modulation, illustrated in Figure 2, a tone frequency ν_t is gated to the the repeller of the klystron at the chopping frequency. Modulation sidebands of frequencies $\nu_0 \pm n\nu_t$ with $n=1,2,3,...$ are generated with intensities decreasing as $1/n^2$. A lock-in amplifier demodulates the detected signal to generate a difference pattern, such as what is illustrated for PH_3 in Figure 3.

Detection was achieved by use of an InSb hot-electron bolometer. The detected signal was demodulated by a lock-in amplifier and converted into digital form. Typically, signal averaging was performed by adding the digitized signal into memory over four upward and four downward sweeps of 256 discrete frequency points, with a lock-in amplifier time constant of 0.3 sec. The spectrum was displayed continuously on an oscilloscope during acquisition. After completion of the specified number of sweeps the spectrum was stored on magnetic disk for future data analysis. On the basis of previous work,[5] the detection sensitivity is 10^{-7} cm^{-1}.

The free-space absorption cell consists of a quartz tube with a cooling jacket surrounded by eight germicidal lamps each capable of producing 5 watts of mercury-line radiation. The lamps are contained within

Figure 2. Frequency spectrum and difference pattern for tone-burst modulation.

TONE BURST MODULATION

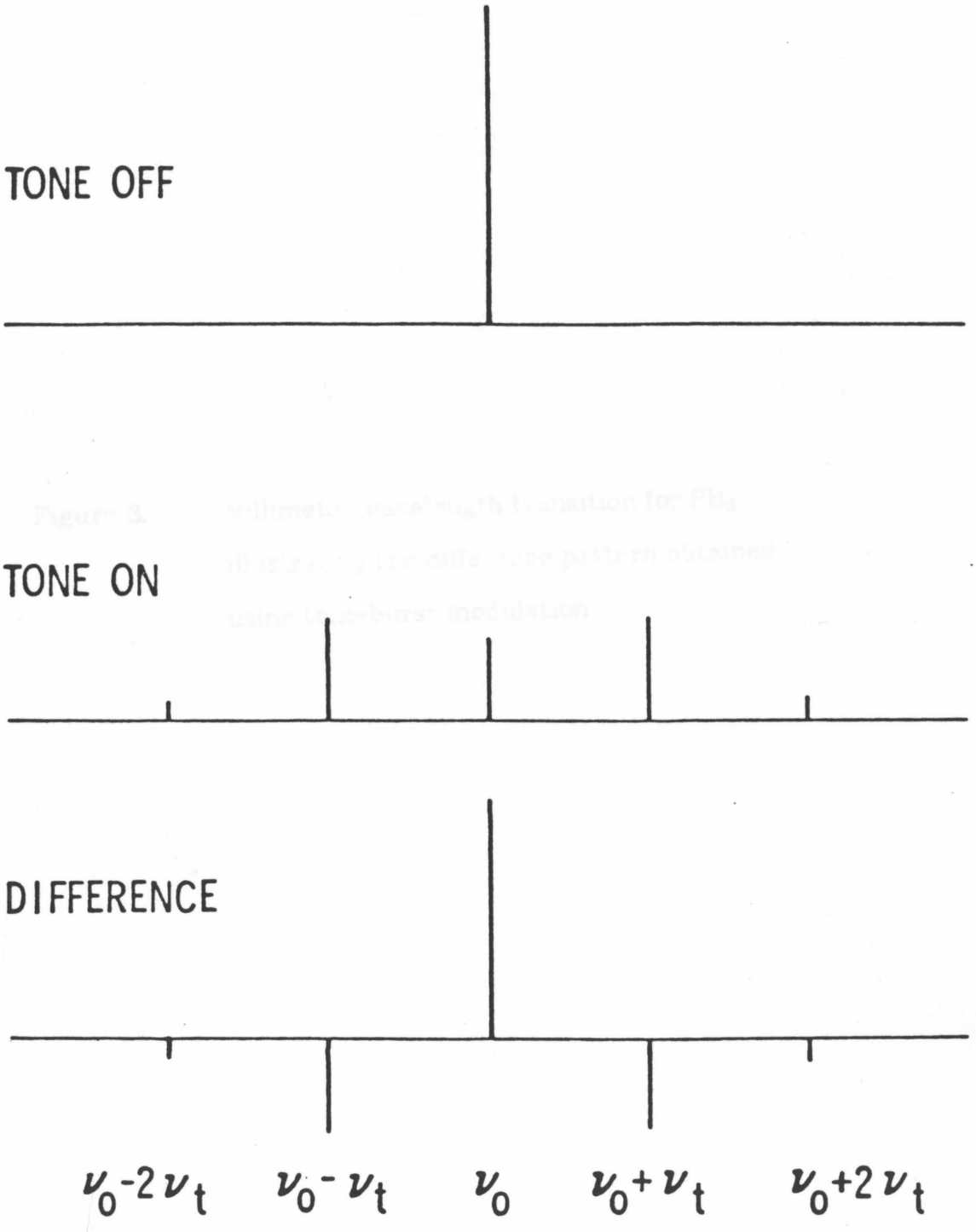

Figure 3. Millimeter wavelength transition for PH_3 illustrating the difference pattern obtained using tone-burst modulation.

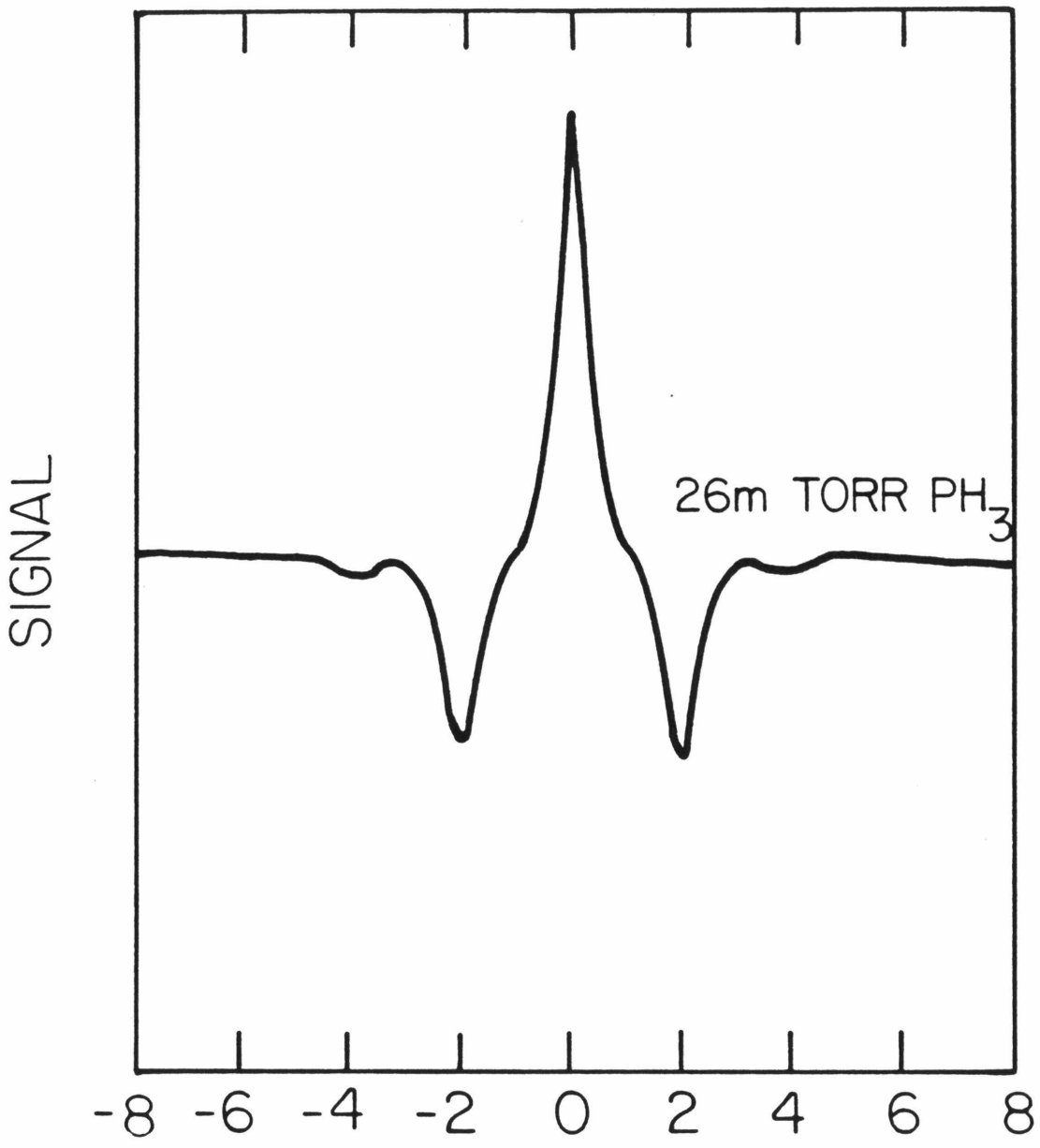
SIGNAL
26m TORR PH3
-8 -6 -4 -2 0 2 4 6 8
FREQUENCY/MHz AT 266944.662 MHz

an aluminum jacket which confines the harmful UV radiation and, when purged with dry N_2, provides a means of preventing frost build-up on the exterior of the cell walls. The sample volume is 3 cm in diameter and 50 cm in length. The cell is cooled by circulating spectroscopic grade methanol through a 10 foot copper coil immersed in a dry ice-isopropanol bath. The chilled methanol passes through the photolysis cell jacket into a dewar reservoir where the temperature is monitored. The circulation of methanol past the photolysis lamps was rapid enough that there is less than a 4K measured temperature differential between the inlet and outlet of the cooling jacket. The end windows of the sample cell were Teflon lenses maintained at room temperature. Mathematical modeling of the temperature gradients in the cell showed that there is a sharp gradient of approximately 2 cm width near the junction of the end caps on the cell with the cooling jacket. Therefore approximately 10% of the sample cell length is at room temperature while the rest of the cell is within 4K of the measured temperature.

Pressure was measured with a Mensor quartz spiral manometer at the exit of the cell. Pressure was also monitored at the inlet to the cell with a thermocouple gauge. Comparison of the two gauges under static conditions and the slow-flow conditions of the experiment showed less than a 1 mtorr differential pressure for flow conditions. The manometer measurements are accurate to ±5 mtorr.

There are several methods by which ClO may be produced in the laboratory. However, the most successful scheme we have found is the photolysis of Cl_2O by mercury-line radiation at 253.7 nm.[6]:

$$Cl_2O \xrightarrow{h\nu} ClO + Cl \qquad k = 0.13\ sec^{-1} \quad (1)$$

The effective first order rate constant is based on 40 watts of 253.7 nm radiation over 425 cm^2 surface area and an absortion cross-section for Cl_2O at this wavelength of 1.9×10^{-18} cm^2. The chlorine atom generated in (1) reacts quickly with another Cl_2O molecule to produce ClO and Cl_2:

$$Cl_2O + Cl \rightarrow ClO + Cl_2 \qquad k = 9.8\times10^{-11}\ cm^3\ molecule^{-1}\ sec^{-1} \quad (2)\ .$$

ClO can react with itself to form a variety of products and is also rapidly photodissociated by the mercury light. Numerical simulation of the photochemistry using the recommended rate constants of Watson[6] suggest that number densities of 5×10^{12} cm^{-3} of ClO would be produced. The observed signal strength is consistent with this estimate.

The approach to measuring linewidths involved first measuring a low-pressure reference spectrum in the Doppler broadened regime. This spectrum contains all the information concerning instrument response and spectral modulation lineshapes in addition to the Doppler contribution to the width. Higher pressure spectra are then obtained by adding the appropriate partial pressure of nitrogen and recording the spectrum under the same spectral resolution and modulation depth conditions present in the low-pressure spectrum. This results in isolating the pressure induced width information when comparison is made between the spectra. The values of the pressure broadening coefficient are obtained by use of a Lorentzian convolution/fitting procedure developed by Pickett.[7] In this work the reference spectrum was taken at pressures below 30 mtorr and well within the Doppler limit. This is done so any changes in reaction chemistry on addition of nitrogen would not change the reference line profile. In fact there did appear to be a small quenching of ClO

production when nitrogen was introduced. Since the Voight profile is a convolution of a Lorentz profile and a Gaussian profile, the convolution procedure permits comparison of Doppler broadened reference spectra with higher pressure spectra which are further into the collision-broadened regime.

III. Results

The upper spectrum in Figure 4 shows a typical low-pressure (30 mtorr) spectrum for the $J = 11/2 \leftarrow 9/2$ transitions of ClO. An example of the $J = 15/2 \leftarrow 13/2$ measurements is given in a previous publication.[7] The spectrum was recorded by tone-burst modulation with a tone frequency of 200 kHz. The lower spectrum in Figure 4 demonstrates the effect of addition of 180 mtorr N_2 to the absorption cell. There are eight distinct lines resulting from nuclear quadrupole splitting and λ-doubling of resulting hyperfine lines. However, under these conditions the λ-doublets are not resolved for the 204 GHz multiplets. The transition frequencies are listed in Table I. The line positions are consistent with predictions based on lower frequency work of Kakar, *et al*.[8] Calculated intensities and frequencies for the lines of ClO are listed on the JPL Submillimeter, Millimeter, and Microwave Spectral Line Catalogue.[9]

Several measurements of linewidth were made at various temperatures and pressures with incident power less than $10\mu Wcm^{-2}$, thus avoiding power saturation. Data is given in Table II. Confidence limits for individual fits of the lineshapes are not given since large correlation between the width and area parameters lead to excessively small uncertainties. In principle, one might expect that there would be some F

Figure 4. Experimental profiles for ClO broadening by nitrogen at 204 GHz. The lower two curves have the same vertical scale.

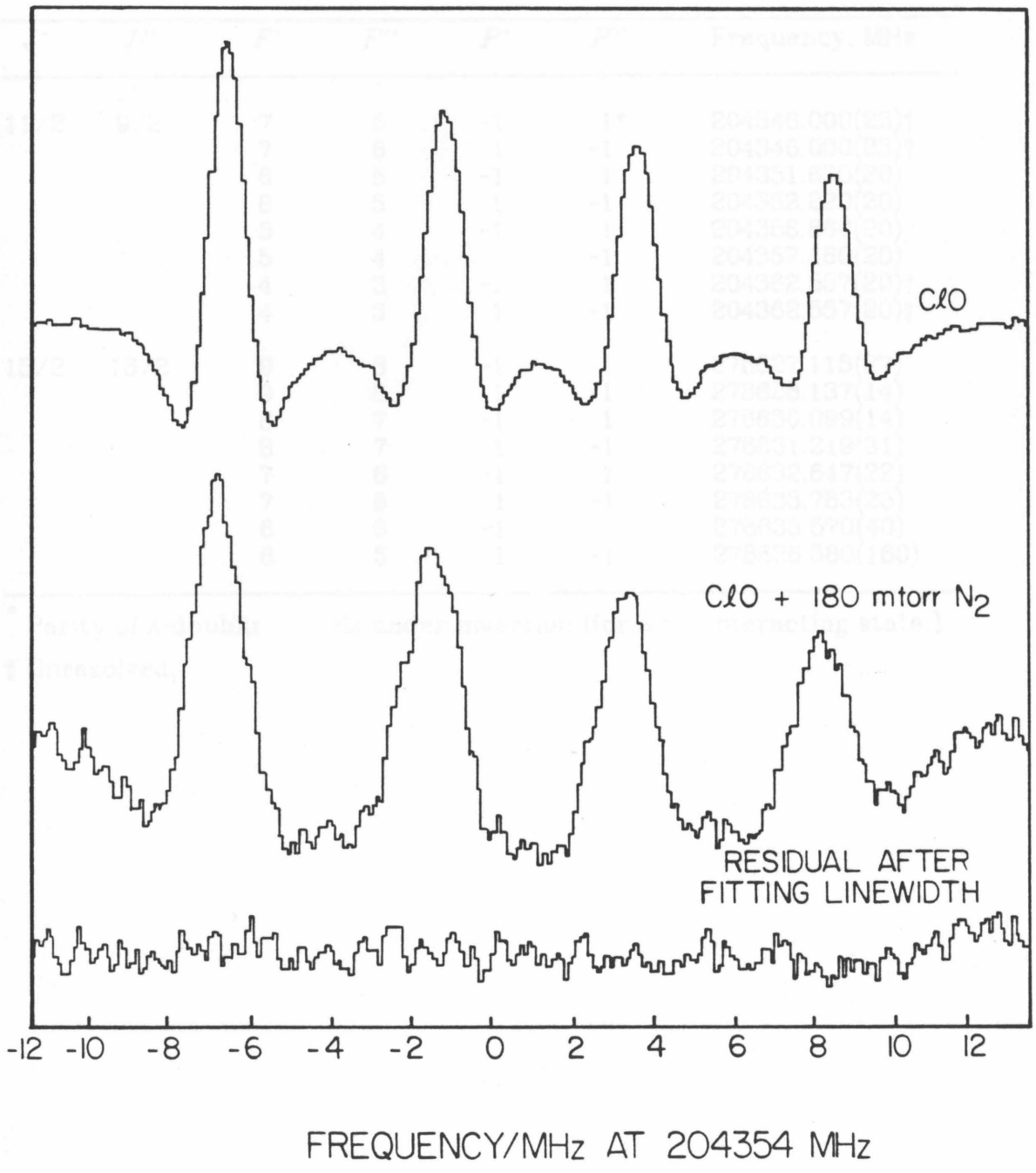
ClO
ClO + 180 mtorr N_2
RESIDUAL AFTER
FITTING LINEWIDTH
-12 -10 -8 -6 -4 -2 0 2 4 6 8 10 12
FREQUENCY/MHz AT 204354 MHz

Table I.

^{35}ClO Line Frequencies Observed for the $^2\Pi_{3/2}$, $v = 0$ Vibronic State

J'	J''	F'	F''	P'	P''	Frequency, MHz
11/2	9/2	7	6	-1	1*	204346.000(23)†
		7	6	1	-1	204346.000(23)†
		6	5	-1	1	204351.630(20)
		6	5	1	-1	204352.220(20)
		5	4	-1	1	204356.860(20)
		5	4	1	-1	204357.480(20)
		4	3	-1	1	204362.557(20)†
		4	3	1	-1	204362.557(20)†
15/2	13/2	9	8	-1	1	278627.115(27)
		9	8	1	-1	278628.137(14)
		8	7	-1	1	278630.099(14)
		8	7	1	-1	278631.219(31)
		7	6	-1	1	278632.647(22)
		7	6	1	-1	278633.783(23)
		6	5	-1	1	278635.570(40)
		6	5	1	-1	278636.580(160)

* Parity of λ-doubling levels under inversion (for a $^2\Sigma^+$ interacting state.)

† Unresolved.

Table II.

Linewidth Measurements

Temperature,K	N_2 Pressure,mtorr	Linewidth Parameter MHz/torr
	204 GHz Multiplet	
218±4	115	4.37
	180	4.70
	235	4.26
		4.44±0.23*
317±4	86	3.08
	100	3.23
	170	3.54
	181	3.40
	295	3.49
		3.35±0.19*
	278 GHz Multiplet	
207±4	50	3.34
	90	4.10
	120	5.09
		4.18±0.88*
317±4	70	3.07
	95	4.29
	144	3.56
		3.64±0.61*
363±10	95	2.86
	151	2.49
	174	2.86
	400	2.44
		2.66±0.23*

* Average.

dependence to the linewidths. However, the procedure used here assumes equal linewidths for each component. Examination of the residuals of the fit in Figure 4 shows that these assumptions are correct to within the accuracy presently available. The higher temperature measurements on the 278 GHz transition of ClO are uncertain by 10K because the measurements were made in an earlier cell which was not thermally controlled. In general the 278 GHz data has larger error bars due to the smaller multiplet splittings which make the transition harder to observe under nitrogen broadening. The pressure broadening coefficients for both transitions are plotted in log-log fashion in Figure 5.

The slope of the curve is such that the presence of room temperature gas in the end of the cell changes the linewidth by 2% and is partially compensated by the temperature gradient in the methanol coolant between the inlet and the measurement point at the outlet of the cooling jacket.

IV. Discussion

The best fit to the data for the 204 GHz multiplet in Figure 5 yields a temperature exponential of -0.75±0.2. Using the arguments found in Townes and Shawlow's book[10] this temperature exponential implies $n=5$ for a $1/r^n$ interaction potential. This is intermediate between dipole-quadrupole ($1/r^4$) and dipole-induced dipole ($1/r^6$) interactions for ClO-N_2 collisions. It is risky to base the temperature exponential on two temperatures and indeed the functional form of a T^x dependence of linewidth on temperature is based on very inexact arguments. Nonetheless it is interesting to note that the dependence

Figure 5. Temperature dependence of ClO broadening by nitrogen.

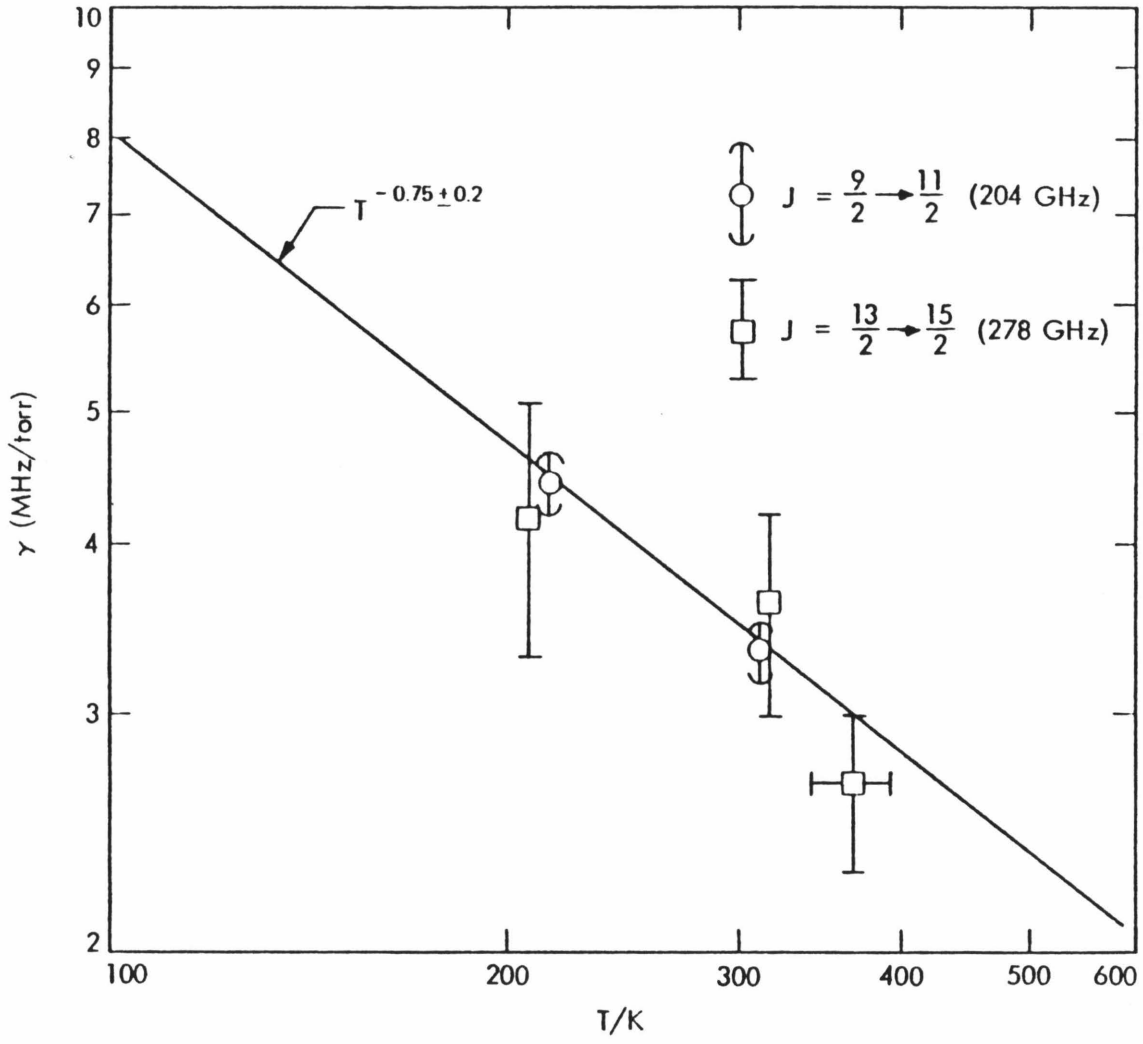
10
9
8
7
6
5
4
3
2
γ (MHz/torr)
100
200
300
400
500
600
T/K
T^-0.75±0.2
J = 9/2 → 11/2 (204 GHz)
J = 13/2 → 15/2 (278 GHz)

obtained is reasonable.

The values obtained here do not alter the conclusions of Waters, *et al.*[2] and were actually used in the analysis of ground-based atmospheric measurements.[3] The values reported here should be useful for future measurements of ClO in both the microwave and infrared regions. We expect that the results should be transferable to infrared transitions involving similar J values. This contention is based on the fact that collisional broadening in both microwave and infrared regions is dominated by rotational energy transfer. The rotational energy transfer in ground and excited vibrational states is different mainly by subtle changes in vibrational averaging of the interaction potential, and should be the same to within 5%. (Currently the measurements reported here form the basis for the linewidths quoted on the Air Force Geophysics Laboratory infrared tapes for the current listing on ClO.)

Acknowledgments.

We would like to thank S. L. Manatt for preparation of the Cl_2O used in this work. Contributions to spectrometer fabrication and maintenance were made by J. C. Hardy and M. M. Schaefer. This research was carried out at the Jet Propulsion Laboratory, California Institute of Technology under contract NAS 7-100 with NASA.

V. References

1. J. A. Logan, M. J. Prather, S. C. Wofsy, and M. B. McElroy, *Phil. Trans. R. Soc. London Ser. A.* **290**, 187 (1978).

2. J. W. Waters, J. J. Gustincic, R. K. Kakar, H. K. Roscoe, P. N. Swanson, T. G. Phillips, T. De Graauw, A. R. Kerr, and R. J. Mattauch, *J. Geophys. Res.* **84**, 7034 (1979).

3. A. Parrish, R. L. deZafra, P. M. Solomon, J. W. Barrett, and E. R. Carlson, *Science* **211**, 1158 (1981).

4. H. M. Pickett, *Rev. Sci. Instrum.* **48**, 706 (1977)

5. H. M. Pickett, E. A. Cohen, and T. G. Phillips, *Astrophys. J.* **236**, L34 (1980).

6. R. T. Watson, *J. Phys. Chem. Ref. Data* **6**, 871 (1977).

7. H. M. Pickett, *Appl. Opt.* **19**, 2745 (1980).

8. R. K. Kakar, E. A. Cohen, and M. Geller, *J. Mol. Spectrosc.* **70**, 243 (1978).

9. R. L. Poynter and H. M. Pickett, *Submillimeter, Millimeter, and Microwave Spectral Line Catalogue*, *Publ. 80-23* Jet Propulsion Laboratory, Pasadena, Calif., (1980).

10. C. H. Townes and A. L. Schawlow, *Microwave Spectroscopy* pp. 368-369, Dover, New York, (1975).

Pressure Broadening of Oxygen and its Implications for Cosmic Background Measurements

H. M. Pickett, E. A. Cohen, and D. E. Brinza

ABSTRACT

The pressure broadening of oxygen transitions at 119 and 425 GHz have been measured in the laboratory for nitrogen and oxygen broadening as a function of temperature. The measured values are significantly different from estimates used by Woody and Richards to obtain a secondary calibration in their cosmic background measurements. The effect of the new determination is to move the calibrated cosmic background further from a Planck function.

I. Introduction

The magnetic-dipole-allowed spin-rotation transitions of molecular oxygen are important for atmospheric absorption in the millimeter and submillimeter wavelength region.[1] The spectrum consists of a multitude of $\Delta J=1$, $\Delta N=0$ transitions near 60 GHz, a $J=1\leftarrow 0$, $N=1$ line at 118.750 GHz, and triplets of $\Delta N=2$ lines spread across the submillimeter region. The latter $\Delta N=2$ lines have zero intensity in the Hund's case *b* limit, but they in fact have appreciable intensity due to mixing of Hund's case *a* basis functions and due to favorable frequency factors in the absorption formulae. Atmospheric absorption from the first set of triplets at 368, 425, and 487 GHz were used as a secondary calibration standard in the balloon measurements of the cosmic background radiation by Woody and Richards.[2] At the time of these balloon measurements, the linewidth parameter for broadening of the oxygen transitions had to be estimated in order to calculate the expected atmospheric emission. Agreement with the measured atmospheric emission was then used to verify that the calibration of received radiation power was being performed correctly during the balloon flight. The frequency dependence of the observed cosmic background had significant deviations from a Planck function, but as they and others[3] have pointed out, a 27% change in calibration would lead to observations which were consistent with a Planck blackbody function.

The measurements reported here were made to obtain laboratory data for the nitrogen and oxygen broadening coefficients of the strongest of the triplets 425 GHz (the $J=2\leftarrow 2$, $N=3\leftarrow 1$ transition). In addition, we report on new measurements for the 119 GHz line. Previous work on the 119 GHz line were made only at room temperature[4], and

here they are extended to lower temperature for both nitrogen and oxygen broadening.

II. Experimental

The measurements were made in a free-space transmission cell which was 3 cm in diameter and 50 cm in length. The cell was constructed with a cooling jacket and was cooled with circulating methanol at a known temperature (within 4K). The end windows were at room temperature, but mathematical modeling of the temperature gradients in the cell showed a sharp gradient in temperature of approximately 2 cm width. Therefore, 10% of the sample cell length is at room temperature while the rest of the cell is within 4K of the measured temperature of the coolant. Pressure was measured to within 10 mtorr by a Mensor QM 300 quartz spiral manometer or by a capacitance manometer which was calibrated against the quartz manometer.

The spectrometer detector was an InSb hot-electron bolometer cooled to 4K. For work at 119 GHz, a klystron was used as a source and was phase-locked and swept under computer control. For work at 425 GHz, the source was the fourth harmonic output of a Schottky diode multiplier driven by the klystron. Tone burst modulation[5] was used for 425 GHz, while measurements at 119 GHz were made with Zeeman modulation and checked with tone burst modulation.

III. Results and Discussion

Spectra, as illustrated in Figure 1, were obtained for pressures ranging from 50 mtorr to 2 torr, and the widths were extracted using the convolution method described previously[5]. The values listed in Table I

Figure 1. Experimental profiles for O_2 self-broadening at 119 GHz. The lower two curves have the same vertical scale.

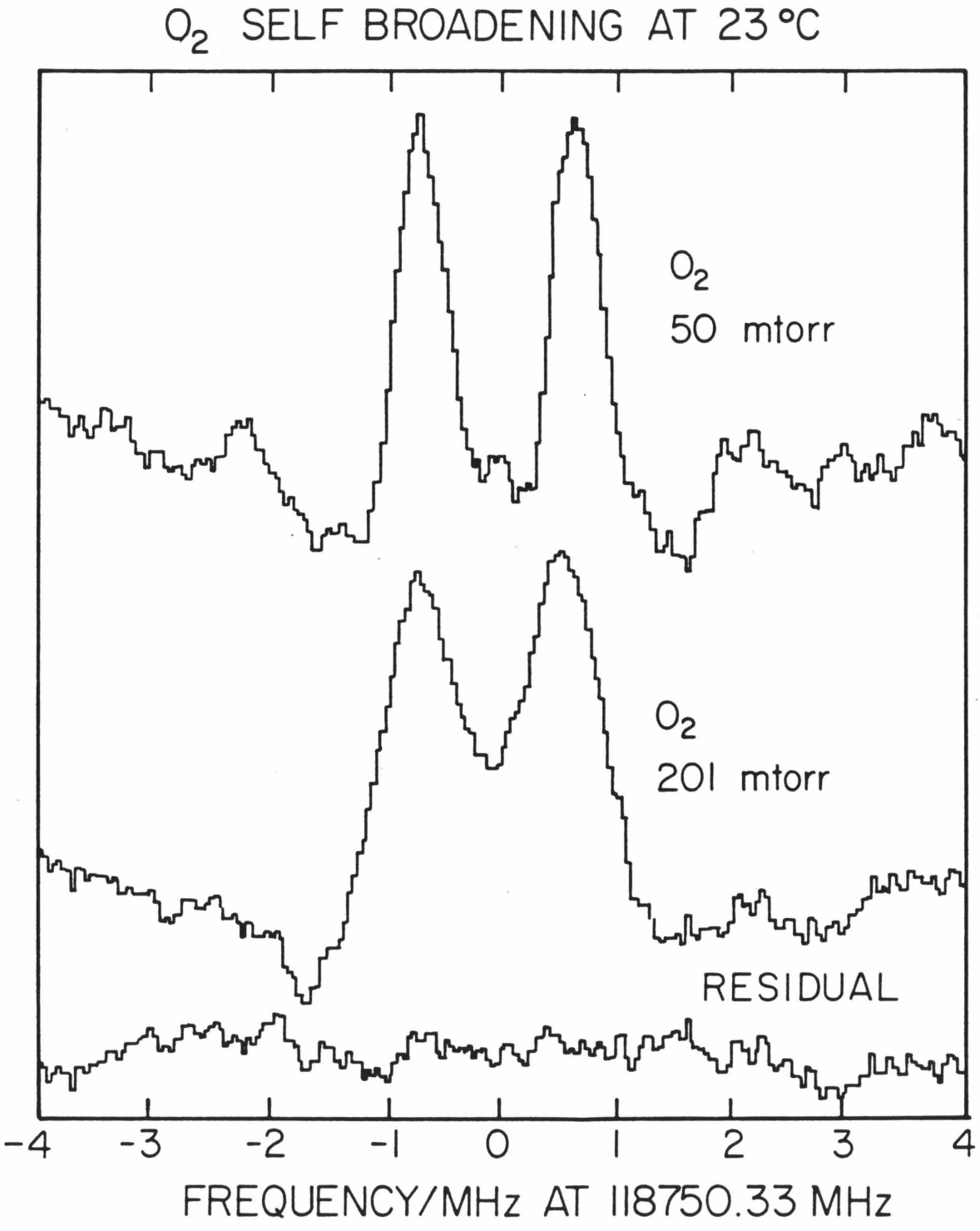
O_2 SELF BROADENING AT 23 °C
O_2
50 mtorr
O_2
201 mtorr
RESIDUAL
-4
-3
-2
-1
0
1
2
3
4
FREQUENCY/MHz AT 118750.33 MHz

Table I.

Pressure Broadening for Oxygen

Transition (GHz)	Broadening Gas	Temperature (K)	Width Parameter (MHz/torr)
119.....	O_2	207	3.05±0.06
119.....	O_2	281	2.30±0.17
119.....	O_2	295	1.98±0.07
119.....	O_2	298	2.13±0.04[a]
119.....	N_2	207	2.83±0.06
119.....	N_2	281	2.38±0.05
119.....	N_2	295	2.2 ±0.10[a]
425.....	O_2	207	2.61±0.26
425.....	O_2	295	1.61±0.16
425.....	N_2	207	2.77±0.24
425.....	N_2	295	2.86±0.31

[a] Setzer and Pickett 1977.

are averages of the width measurements, and the error estimates are the standard deviation of the measurements from the average. The measurements at 425 GHz were difficult because the power levels were low, because the line is weak (making the baseline more prominent), and because the line has a large splitting (~3 MHz) in the Earth's magnetic field. The latter problem is particularly acute because the g-values for the upper and lower states are -0.6363 and 0.9702, respectively. The widths are certainly preliminary, and significant improvements can be made in measurement accuracy and sensitivity by cancellation of the Earth's magnetic field in the laboratory.

The data on widths for the transitions present interesting similarities and contrasts. Nitrogen broadening at 119 GHz follows a temperature dependence which is expected on the basis of simple semiquantitative arguments [6,7], namely, $T^{-0.7\pm0.2}$ experimentally versus $T^{-0.75}$ for a quadrupole-quadrupole potential, and $T^{-0.7}$ for a van der Waals potential. For the 425 GHz line, the nitrogen broadened width seems to decrease with temperature; however, the error estimates are consistent with a temperature exponent of 0.1± 0.6. As can be seen in Figure 2, oxygen self-broadening has a much stronger temperature dependence ($T^{-1.2}$) than nitrogen broadening. One qualitative explanation for the steeper dependence is that the self-broadening width contains contributions from both inelastic processes and from resonant exchange processes. Recently evidence for resonant exchange has been observed for HCl self-broadening[8]. In oxygen, the exchange or spin-flip process will be mediated by a magnetic-dipole interaction between the electron spins, and the temperature dependence of exchange broadening will be T^{-1} times the temperature-dependent probability that the colliding molecule is in a

Figure 2. Temperature dependence of O_2 self-broadening and broadening by nitrogen.

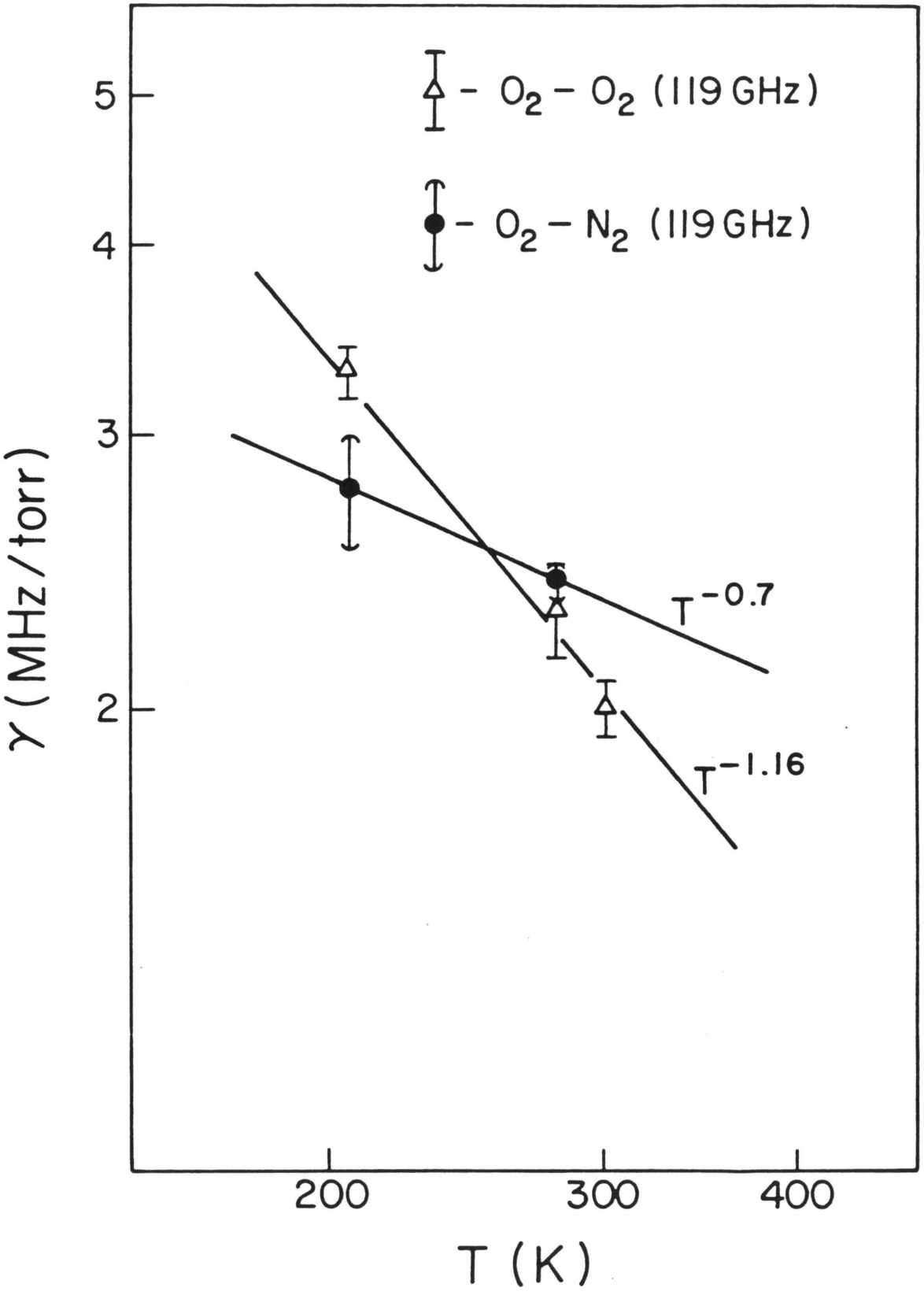
- $O_2 - O_2$ (119 GHz)
- $O_2 - N_2$ (119 GHz)
$T^{-0.7}$
$T^{-1.16}$
γ (MHz/torr)
T (K)
5
4
3
2
200
300
400

state which has transitions to levels with nearly the same frequency as the observed frequency[9]. For the 119 and 425 GHz lines, this probability will be inversely proportional to temperature, for a total temperature dependence for exchange of T^{-2}. The observed temperature dependence is intermediate between T^{-2} for the exchange process and $T^{-0.7}$ for inelastic scattering. This qualitative explanation is also consistent with the smaller self-broadening coefficient at 425 GHz line than the 119 GHz line. The evidence for exchange in the temperature dependence of widths would not be as apparent in the broadening of 60 GHz lines, since virtually every oxygen collision partner can undergo resonant exchange.

The impact of the measurement reported here on the experiment of Woody and Richards[2] is not completely clear at the present time because of a number of other factors which were not treated thoroughly in the original calculation, the most significant being the effects of Zeeman broadening on absorption which depends on the orientation of the observation direction with respect to the Earth's field[3]. Taken by itself, however, the air-broadened width at 425 GHz is 2.67 ± 0.2 MHz torr^{-1} from this work, compared with an earlier estimate of 1.9 MHz torr^{-1} based on an average of room temperature values for the 1^+ and 3^- line widths at 60 GHz[10]. Since the oxygen lines are saturated under the conditions of the balloon experiment, observed emission from the balloon is proportional to the square root of the width[2]. The effect of this new width determination is therefore to move the calibrated cosmic background 20% ***further*** away from a Planck function.

This work was carried out at the Jet Propulsion Laboratory of the California Institute of Technology under contract NAS7-100 with NASA.

IV. References

1. J. W. Waters, *Methods of Experimental Physics*, Vol. **12,** *Astrophysics*, Part B, pp. 142-176 (1976).

2. D. P. Woody and P. L. Richards, *Phys. Rev. Letters* **42,** 925 (1980).

3. R. Weiss, *Ann. Rev. Astr. Ap.* **18,** 489 (1980).

4. B. J. Setzer and H. M. Pickett, *J. Chem. Phys.* **67,** 340 (1977).

5. H. M. Pickett, *Appl. Optics* **19,** 2745 (1980).

6. C. H. Townes and A. L. Schawlow, *Microwave Spectroscopy* pp. 368-369, Dover, New York (1975).

7. H. M. Pickett, *J. Chem. Phys.* **73,** 6090 (1980).

8. M. Zughul, J. Gelfand, H. Rabitz, and A. E. DePristo, *J. Quant. Spectrosc. Rad. Transf.* **24,** 371 (1980).

9. H. M. Pickett, *J. Chem. Phys.* **63,** 2153 (1975).

10. H. J. Liebe, G. G. Gimmestad, and J. D. Hopponen, *IEEE Trans.* **AP-25,** 327 (1977).

Chapter II

Millimeter Microwave Spectroscopy of CS Produced in the ArF Excimer Laser Photolysis of CS_2

Millimeter Microwave Spectroscopy of CS Produced in the ArF Excimer Laser Photolysis of CS_2

D. E. Brinza, K. C. Janda, and H. M. Pickett

ABSTRACT

A transient microwave absorption spectrometer, designed for the observation of short-lived radicals formed by pulsed laser photolysis, is described. Attempts were made to measure the rotational spectra of CS($X^1\Sigma^+$, v''=0–5) produced in the photodissociation of CS_2 by an ArF excimer laser. The inability to observe microwave spectra of the direct photoproducts is attributed to unfavorable translational and rotational relaxation rates at high fragment velocities.

I. Introduction

Excimer laser systems, characterized by relatively high pulse energies and wavelength specificity, make excellent flash photolysis light sources. With such laser systems, a specific amount of energy may be deposited within a molecule. If this amount of energy exceeds the dissociation energy of chemical bonds within the molecule, the molecular dynamics of the photodissociation may be investigated. In the case of large molecules, the final products of photodissociation may be various chemical species. For example, the KrF laser (248 nm) photolysis of $Fe(CO)_5$ in the gas phase[1] yields approximately 55% $Fe(CO)_2$, 35% $Fe(CO)_3$ and 10% $Fe(CO)_4$ as determined by trapping the photoproducts with PF_3. This result is in contrast to the solution phase photolysis of $Fe(CO)_5$[2] which almost exclusively results in the loss of only one carbonyl group. Photolysis by excimer lasers leads to distribution of energy into vibrational, rotational and translational degrees of freedom of the fragments which, for some molecules, have been determined experimentally. Such a measurement, performed upon the ArF laser (193 nm) dissociation of CS_2, is described in some detail below.

Quite often, the reactivity of a particular radical with its precursor molecule is so great that microwave spectra cannot be obtained for that radical species. The number density of radicals obtained in traditional methods of generation (i.e. microwave discharge or c.w. radiation) is often insufficient to permit measurable absorption of microwave power. The use of an excimer laser as a photolysis source introduces the possibility of destroying essentially all of the precursor molecules, creating very high initial concentration of radical species. These radicals can then undergo sufficient collisions with buffer gas molecules in order to relax

and give rise to a transient microwave absorption. The CS radical was selected as a trial molecule since it is long-lived (≫1 sec) its microwave spectrum is known[3,4] and the precursor molecule has a very large cross-section ($\varepsilon \sim 50{,}000$ l mole^{-1} cm^{-1}) for photodissociation at 193 nm.

Detailed information concerning the translational and internal energy distributions of the CS fragment from photolysis of CS_2 at 193 nm was obtained by Bersohn, *et.al.*[6]. Two electronic channels are energetically accessible to the CS and S fragments from the photodissociation. The S atom may be produced in either the ^3P ground state or the ^1D excited state but there is insufficient energy to produce electronically excited CS ($A^1\Pi$). The translational energy distribution, as determined from the time-of-flight spectrum of the CS fragment, indicates approximately 80% of the S atom is produced in the ^1D state. Laser-induced fluorescence spectra of the CS($v \leq 6$) fragment, led to the finding that the $v=3$ and 4 levels are predominately formed in the photodissociation process. The CS fragment was observed to have considerable rotational energy, the $A^1\Pi - X^1\Sigma^+$ (5-4) vibronic band indicating an average J of ~40 for the fragment. The system is thus characterized such that the velocity of a fragment CS(v,J) can be calculated from conservation of energy and momentum.

The current study attempts to exploit this detailed knowledge of the energetics of CS_2 photodissociation process in order to determine the limits of relaxation that can be expected under pressure conditions suitable for microwave studies ($P_{total} < 1$ torr). Section II describes the transient microwave absorption spectrometer. Section III reports the observation of CS only in the $v=0$ state. The existence of the CS ($v=0$) radical is shown to be due to secondary chemistry of the S atom with CS_2.

Failure to see evidence of the direct photoproducts is argued to be caused by diffusion of the radical out of the absorption cell before rotational relaxation occurs.

II. Experimental

The transient microwave absorption spectrometer is shown schematically in Figure 1. The millimeter microwave source, capable of producing microwaves in the 80-800 GHz range, has been previously described.[7] Pulses (~100mJ) from a Lumonics Model 861-S excimer laser operating with ArF were directed through quartz windows into a 1 meter path length fast flow cell. The rectangular laser beam (8 mm × 25 mm) illuminates approximately 40% of the cell volume. The ultraviolet and microwave radiations were coupled into the flow cell by means of a fine wire mesh. The 200 grid per inch nickel mesh is 90% transparent to optical wavelengths and essentially 100% reflective for millimeter microwaves. The polarization vector of the microwave $TE_{1,0}$ mode was oriented in such a manner as to maximize the overlap of its intensity with the excimer beam. An InSb bolometer at 4K was used to detect the transmitted microwave power. The signal was amplified by a low-noise FET input preamplifier. The time dependent signal was captured by a multi-channel signal averager (MCSA). RF interference from the excimer laser was severe, necessitating the enclosure of the nV sensitivity detection electronics within a Faraday case. The entire spectrometer is controlled by a microcomputer system.

In a typical data acquisition cycle, the microcomputer first triggers the MCSA, then, after a fixed delay (~250 μsec) triggers the excimer. If the microwave source is tone-burst modulated,[8] the triggering of the averager and excimer laser is synchronized to the gating of the

Figure 1. Diagram of the transient microwave absorption spectrometer.

MILLIMETER SPECTROMETER FOR MEASUREMENT OF ABSORPTION BY PHOTOCHEMICAL TRANSIENTS

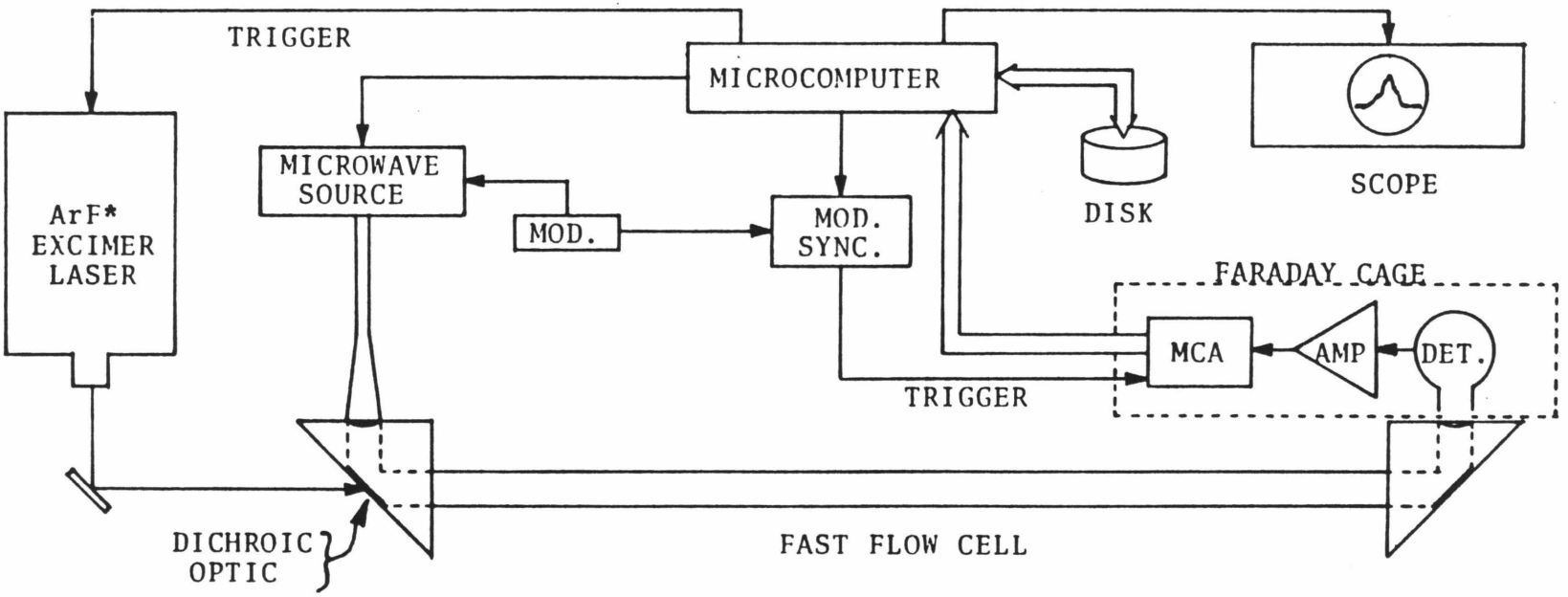

frequency modulation. The transient absorption signal is thus averaged for a pre-determined number of laser pulses, after which the computer reads the contents of the MCSA. An example of the unmodulated transient microwave absorption for the $J=4\leftarrow3$ transition of CS($v=0$) is shown in Figure 2. The apparent decay for the CS absorption signal is not related to the lifetime of CS, rather it is due to the bandpass characteristics of the preamplifier. The persistence of the CS radical is demonstrated in the tone-burst modulated transient waveform shown in Figure 3. Here the tone-burst modulation has the effect of gating the microwave frequency on and off the resonance frequency, resulting in the modulated transient absorption.

III. Results and Discussion

The CS($v=0$) $J=4\leftarrow3$ spectrum shown in Figure 4 was obtained by scanning the klystron forward and backward over the frequency region twice. Each frequency point in the spectrum was averaged for 80 laser shots, equivalent to an effective time constant of 16 msec. The spectrum appears as a Lorentzian line shape centered at 195,954.188 MHz with a FWHM of 1.2 MHz. The observed center frequency is well-within the error limits for the previously reported $J=4\leftarrow3$ transition frequency[3] of 195,954.162±0.050 MHz. The 1.2 MHz linewidth corresponds to a collisional frequency of 7.5×10^6 sec^{-1}.

All attempts to observe the transient microwave absorption spectra for vibrationally excited CS ($v\leq5$) were unsuccessful. In view of the vibrational distribution reported by Bersohn[6] and noting that the dipole moment of CS changes only slightly[9] for $v=1$ (1.936 D) compared to $v=0$ (1.958 D), the microwave spectra of the vibrationally excited species were expected to be considerably more intense than the $v=0$

Figure 2. Unmodulated transient absorption scan for the $J = 4 \leftarrow 3$ transition of $CS(X, v'' = 0)$.

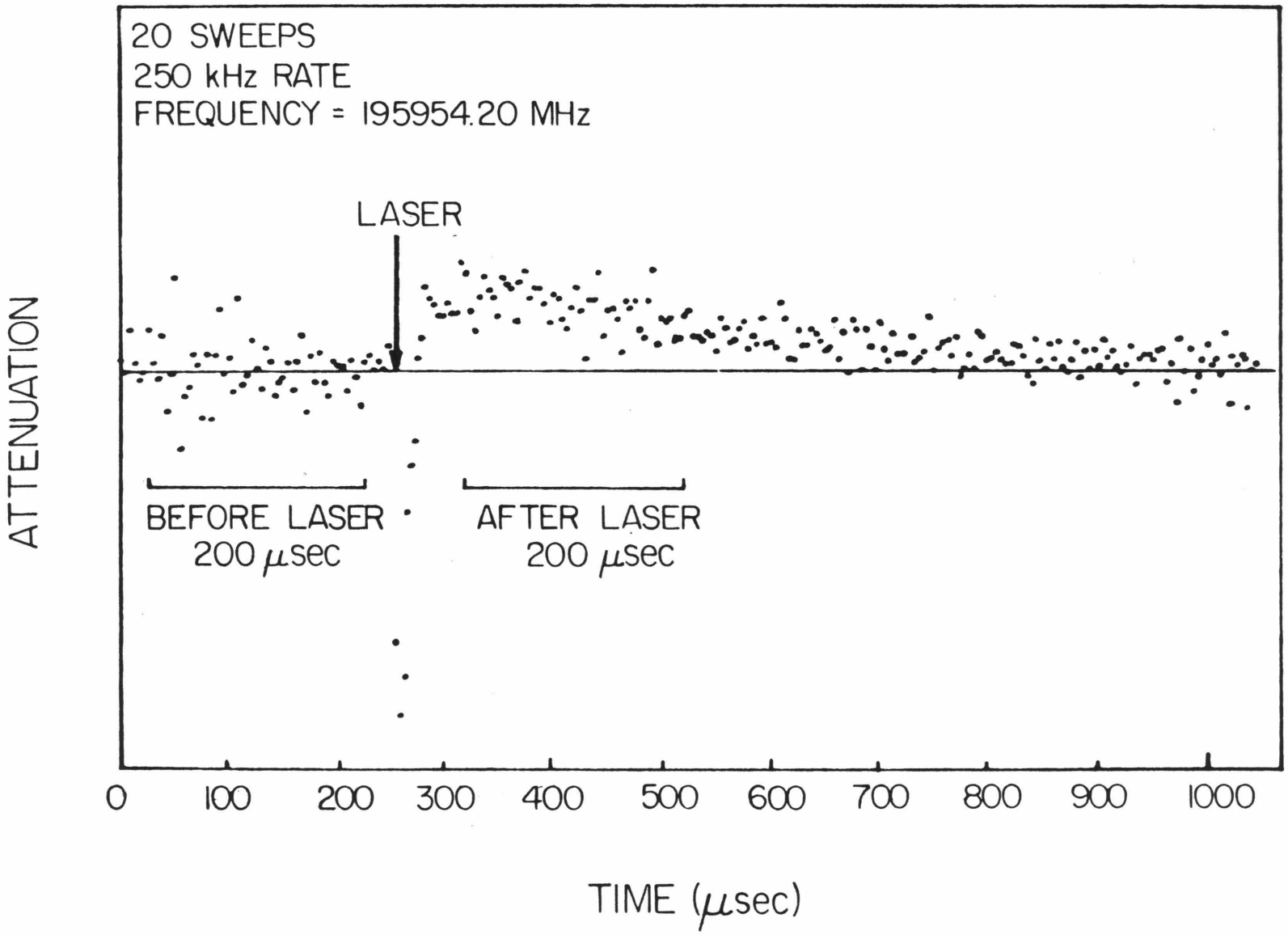
20 SWEEPS
250 kHz RATE
FREQUENCY = 195954.20 MHz
LASER
BEFORE LASER
200 μsec
AFTER LASER
200 μsec
ATTENUATION
0
100
200
300
400
500
600
700
800
900
1000
TIME (μsec)

Figure 3. Modulated transient absorption scan for the $J = 2 \leftarrow 1$ transition of CS.

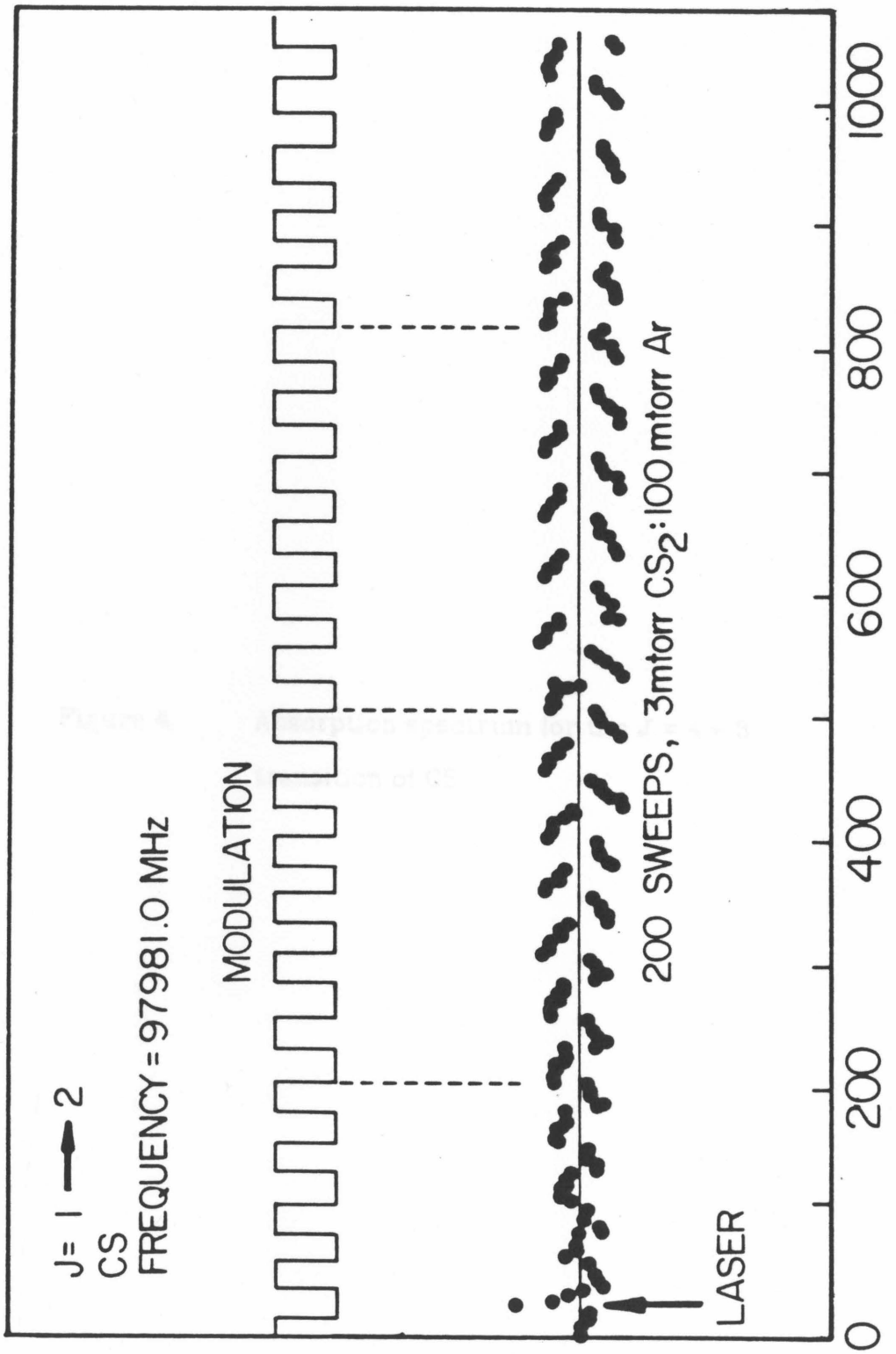
J= 1 ← 2
CS
FREQUENCY = 97981.0 MHz
MODULATION
200 SWEEPS, 3mtorr CS_2: 100 mtorr Ar
LASER
0
200
400
600
800
1000
μsec

Figure 4. Absorption spectrum for the $J = 4 \leftarrow 3$ transition of CS.

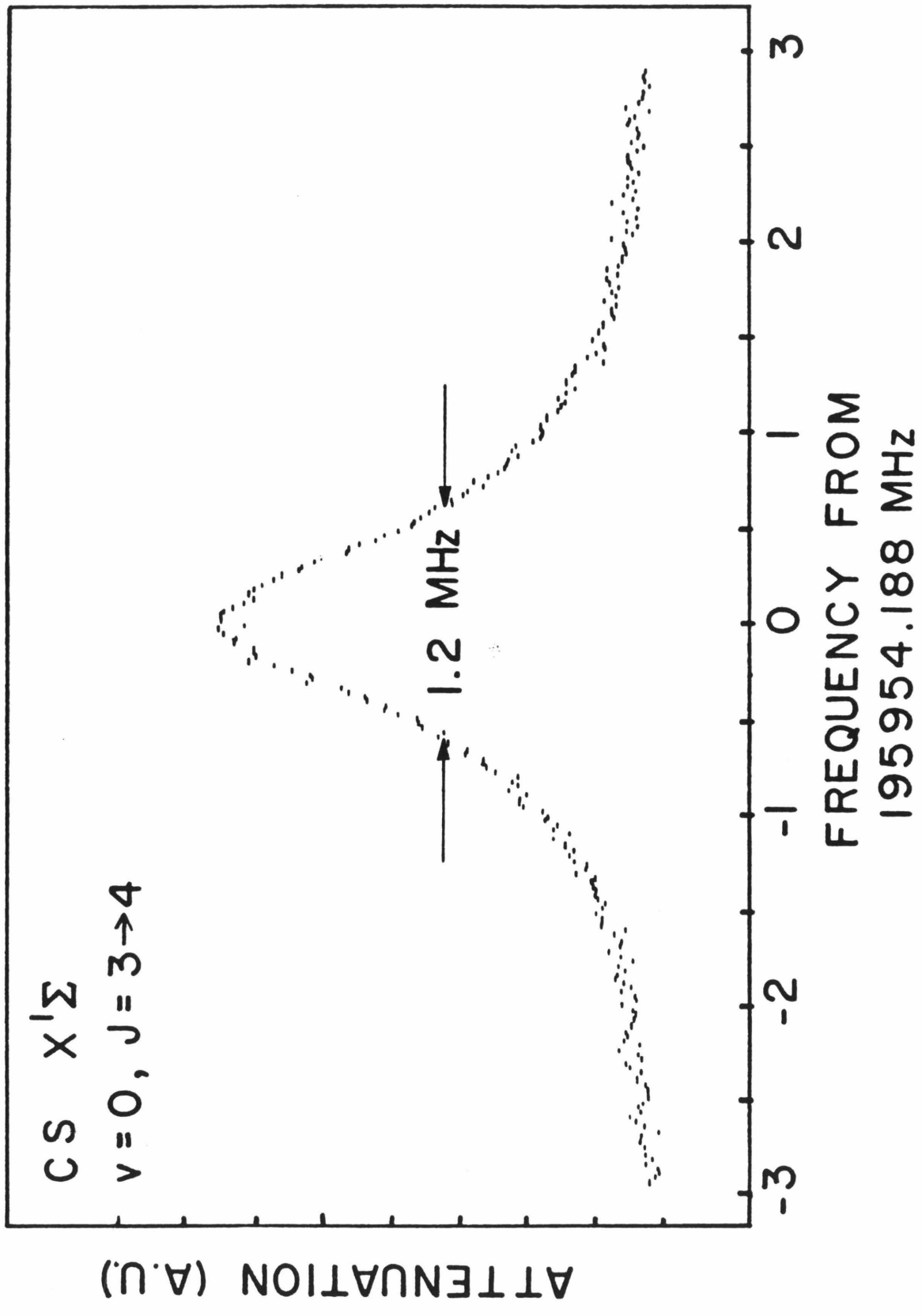
CS X¹Σ
v=0, J=3→4
1.2 MHz
-3
-2
-1
0
1
2
3
FREQUENCY FROM
195954.188 MHz
ATTENUATION (A.U.)

spectrum. There are two plausible explanations for the observation of only CS(v=0) by microwave spectroscopy:

1) The vibrationally excitation of the CS radicals is efficiently quenched in collision with S atom, CS and CS_2 in the cell, and

2) The CS fragments produced in the photodissociation diffuse out of the absorption path before becoming rotationally relaxed.

Explanation 1) seems indeed quite reasonable since the early work of Callear[10] suggests rapid vibrational quenching of CS (v>0) by S atom, possibly involving multiple quantum transitions. Explanation 2), as stated above, does not explain the observation of the CS(v=0) microwave absorption.

The question as to whether the vibrationally excited CS is being quenched after formation can be addressed experimentally by lowering the partial pressure of CS_2 in the cell. As the relative number of quenching species is decreased, the rate of quenching should similarly decrease. The v=0 intensity should decrease, while the vibrationally excited spectra should increase in intensity. Such experiments were performed, decreasing the partial pressure of CS_2 to the point where no CS(v=0) was observed. There were no indications of vibrationally excited CS in any of the measurements. Under typical conditions (100-300 mtorr Ar, 3 mtorr CS_2), the CS or S fragments will undergo tens of collisions with the Ar atoms before striking the wall or diffusing out of the cell. There should be essentially no collisions between radical species in this time scale (<100 μsec). This seems to suggest that the quenching process may not be responsible for the failure to observe vibrationally excited photofragments.

The other possibility is the rapid diffusion of CS from the cell as compared to the rate of rotational relaxation. For the sake of a numerical example, the energetics of the process:

$$CS_2 \xrightarrow{h\nu} CS(X^1\Sigma^+, v=3, J=40) + S(^1D) + E_{trans}$$

is considered. The excess energy available to vibrational, rotational and translational degrees of freedom for the dissociative channel with $CS(X^1\Sigma^+, v=J=0)$ and $S(^1D)$ is approximately 7,000 cm^{-1} for ArF excitation of CS_2. Using the constants for CS in Herzberg,[11] approximately 5,000 cm^{-1} appears as internal energy for CS ($v=3$, $J=40$) with over 1200 cm^{-1} in the rotational degrees of freedom. The remaining 2000 cm^{-1} of excess energy appears as relative translational kinetic energy in the CS and S fragments. Applying the conservation of momentum and energy leads to a CS fragment velocity on the order of $7.\times10^4$ cm/sec. Since the effective collisional cross-section for rotational energy transfer decreases at higher molecular velocities, and there is a considerable amount of rotational energy to be removed from the fragment, it seems probable that the excited CS would diffuse from the cell while still in a high J state.

What about the observed microwave spectrum for $CS(v=0)$? To this point, the S atom has only been considered as a spectator removing excess energy in the form of electronic excitation and/or translational kinetic energy. Yet S atom is known to react very rapidly with CS_2 to yield CS and S_2[12]:

$$S + CS_2 \rightarrow CS + S_2 \quad k = 2.5\times10^{-11}\ cm^3\ s^{-1}\ .$$

The ΔH for the reaction is only approximately -9 kcal $mole^{-1}$, resulting in $CS(v=0)$ as the most likely product. The fact that the products are both diatomics allow the heat of reaction to be distributed over the rotational

degrees of freedom for both species. Therefore the excitation within the CS may not be large. A simple kinetic model, using the calculated number densities of the species present in the cell after the laser pulse and the above quoted rate constant, was tested. The number density of CS formed in the S + CS_2 reaction reaches 90% of its final value within 200 μsec after the laser pulse. This is in good agreement with the build up of CS microwave absorption witnessed in the modulated transient absorption scan (Figure 3).

The suggestion that the observed CS (v=0) is formed by the action of S atom upon CS_2 can be more conclusively tested. Sulfur atoms are known to react readily with olefins to produce thiiranes, which are the sulfur analogs of epoxides. Furthermore, S (^{1}D) can insert between the vinylic C-H bond to yield vinylic mercaptans. The quoted bimolecular rate constants:[13,14]

$$S(^1D) + C_2H_4 \rightarrow \underset{\diagdown\ S\ \diagup}{H_2C\text{—}CH_2} \qquad k = 3\times10^{-11}\ cm^3\ s^{-1}$$

$$S(^3P) + C_2H_4 \rightarrow \underset{\diagdown\ S\ \diagup}{H_2C\text{—}CH_2} \qquad k = 2\times10^{-12}\ cm^3\ s^{-1}$$

imply that a large excess ethylene will scavange the S atoms, inhibiting the formation of CS. In the photolysis of 3 mtorr CS_2 in ~100 mtorr ethylene, virtually no CS (v=0) microwave absorption could be detected.

In conclusion, the following observations concerning the feasibility of measuring microwave spectra of direct photoproducts are made:

1) The translational and internal (in particular, rotational) energy distributions may be unfavorable in terms of permitting sufficiently rapid relaxation.

2) There is a point of diminishing returns in regards to increasing the buffer gas pressure to hasten relaxation, and that is, the transition may be collisionally broadened to such an extent as to become virtually unobservable.

3) The observation of the spectrum for the species of interest is not necessarily an indication of the success of a proposed scheme. Secondary reaction may cause formation of the species of interest with an entirely different distribution of energy among the degrees of freedom than what would be encountered in the direct photofragments.

The third point above is probably of least worry to the spectroscopist charged with the observation of the particular species. In some cases, the secondary chemistry is one of the major sources of the radical species to be measured, for example, ClO[7]. Transient microwave absorption spectroscopy may have application in the study of chemical kinetics, but its use as a probe for determining product state distributions does not seem feasible.

This work was carried out at the Jet Propulsion Laboratory, California Institute of Technology, under the Presidents Research Fund.

IV. References

1. G. Nathanson, B. Gitlin, A. M. Rosan, and J. T. Yardley, *J. Chem. Phys.* **74,** 361 (1981).

2. M. Wrighton, *Chem. Rev.* **74,** 401 (1974).

3. R. Kewley, K. V. L. N. Sastry, M. Winnewisser, and W. Gordy, *J. Chem. Phys.* **39,** 2856 (1963).

4. F. J. Lovas and P. H. Krupenie, *J. Phys. Chem. Ref. Data* **3,** 245 (1974).

5. J. W. Rabalais, J. M. McDonald, V. Scherr, and S. P. McGlynn, *Chem. Rev.* **71,** 73 (1971).

6. S. C. Yong, A. Freedman, M. Kawasaki,, and R. Bersohn, *J. Chem. Phys.* **72,** 4058 (1980)

7. H. M. Pickett, D. E. Brinza, and E. A. Cohen, *J. Geophys. Res.* **86,** 7279 (1981).

8. H. M. Pickett, *Appl. Optics* **19,** 2745 (1980).

9. M. Winnewisser and R. L. Cook, *J. Mol. Spectrosc.* **28,** 266 (1968).

10. A. B. Callear, *Proc. Roy. Soc. (London) Ser A* **276,** 401 (1963).

11. G.Herzberg, *Molecular Spectra and Molecular Structure, Volume I. Spectra of Diatomic Molecules, 2nd ed.* Van Nostrand Reinhold, New York (1950).

12. N. Basco and A. E. Pearson, *Trans. Farad. Soc.* **63,** 2684 (1967).

13. O. P. Strausz, W. B. O'Callaghan, E. M. Lowm and H. E. Gunning, *J. Amer. Chem. Soc.* **93,** 559 (1971).

14. O. P. Strausz, *Sulfur Research Trends*, *Adv. in Chem. Ser.*, *Vol. 110*, Amer. Chem. Soc., Washington D. C., pg.139 (1972).

Chapter III

Molecular Beam - Laser Spectroscopy of Ne-Cl_2 : Observation of a Metastable Vibrationally Excited van der Waals Molecule

Molecular Beam - Laser Spectroscopy of $Ne-Cl_2$: Observation of a Metastable Vibrationally Excited van der Waals Molecule

D. E. Brinza, C. M. Western, B. A. Swartz, and K. C. Janda

ABSTRACT

Laser-induced fluorescence excitation spectra of expansions containing He, Ne, and Cl_2 were obtained with a new pulsed molecular beam apparatus and excimer-pumped dye laser system. Spectroscopic features observed ~6 cm^{-1} to the blue of the (4-0) through (16-0) and the (8-1) through (11-1) vibronic origins of the $B-X$ system of Cl_2 have been attributed to the van der Waals molecule $Ne-Cl_2$. Fitting of the computed band shape to the observed data indicates that $Ne-Cl_2$ is a T-shaped molecule with a Ne to Cl_2 center-of-mass separation of ~3.6 Å in the ground state. Of particular interest is the observation of Ne bound to Cl_2 ($X^1\Sigma_g^+$, $v''=1$), since the Cl_2 vibrational energy (~560 cm^{-1}) far exceeds the van der Waals bond strength (<70 cm^{-1}). A **lower** bound of 10^{-5}s has been placed upon the lifetime of this metastable complex, based on the time-of-flight from the nozzle to the laser interaction region. The observation of "hot-band" $Ne-Cl_2$ lends strong support to "energy-gap" and "momentum-gap" theories which predict long-lived vibrationally excited triatomic van der Waals molecules.

I. Introduction

The vibrational predissociation of van der Waals molecules has become a very active area in experimental and theoretical chemical physics. Supersonic molecular beam techniques, coupled with high-resolution dye lasers, have made possible the preparation and spectroscopic determination of vibrational predissociation rates of van der Waals molecules in a collision-free environment. The wide disparity in energy, hence weak coupling, between the vibrational modes of chemically bound species and the van der Waals vibrational modes in a small van der Waals molecule permits the preparation of a well-defined excited state of the complex by a laser. If vibrational energy in excess of the van der Waals binding energy is deposited within the complex upon excitation, the energy will be redistributed within the complex, eventually leading to dissociation. The unimolecular decomposition generally proceeds on a single potential energy surface. The dissociation energy of the van der Waals bond is generally much less than the energy required to break typical covalent bonds. Therefore the vibrational predissociation of van der Waals molecules is a comparatively simple process, providing models for detailed theoretical investigations into the dynamics of dissociation and intramolecular energy transfer.

The elegant series of laser-molecular beam experiments performed by the Levy group[1-7] have provided considerable insight into the structure and dynamics of small van der Waals molecules. Iodine, with its strongly fluorescent $B-X$ system and relatively long fluorescence lifetime ($\sim$1 μsec) has proved to be an ideal molecular substrate for the preparation of well-defined excited states of van der Waals species by laser excitation. Under the conditions of a supersonic expansion with

approximately 1 ppm I_2 in He, the van der Waals molecule He-I_2 was identified as the species responsible for bands occuring 3.4 - 4.0 cm^{-1} to the blue of the (3-0) through (29-0) I_2 vibronic bandheads.[1] The rotational structure of the He-I_2 band was analyzed[2] yielding a *T*-shaped structure for the complex. Analysis of the line shape of the R-branch head (high-frequency side) of the He-I_2 bands by fitting to a Lorentzian function yielded predissociation lifetimes[3] ranging from 220ps for the (12-0) band down to 38ps for the (26-0) bands. The vibrational predissociation rate was found to be empirically described by a quadratic plus cubic dependence in upper state vibrational quantum number. The dispersed fluorescence spectrum of He-I_2 ($B,v'=22$) was dominated by transitions from I_2 in the $v'=21$ state[4] giving rise to the propensity rule $\Delta v=-1$ for the vibrational predissociation process. Studies of complexes of I_2 with Ne and He[5] gave rise to the "band-shift rule" in which the position of complexes of the type $I_2Ne_aHe_b$ relative to the uncomplexed I_2 bandhead is given by the simple formula

$$\nu_{I_2Ne_aHe_b} - \nu_{I_2} = a \cdot A + b \cdot B \ (cm^{-1})$$

where the coefficients *A* and *B* depend weakly on the I_2 *B*-state vibrational quantum number. In the larger complexes, i.e. I_2Ne_6, the propensity rule $\Delta v=-1$ (per rare gas atom dissociated) breaks down, requiring a few extra vibrational quanta to remove all of the rare gas atoms. This breakdown seems to indicate a statistical redistribution of the energy of I_2 vibration among the many van der Waals bending modes, thus affecting dissociation with less than unit efficiency. Similar results were obtained for complexes of I_2 with Ar and He[6], with each Ar atom producing a band shift of about 13.5 cm^{-1} to the blue of the I_2 vibronic bandhead. Complexes with more than three Ar atoms, though, were not observed,

possibly due to electronic predissociation of I_2 induced by the Ar atoms. Three or more quanta of I_2 vibrational energy were required to remove each Ar atom from the complex excited to the (21-0) level. The rotational state distribution, as determined from the dispersed fluorescence band shape of the I_2 fragment from the vibrational predissociation of Ar-I_2 (21-0), indicates that as much as 10 percent of the energy (~150 cm^{-1}) in excess of the van der Waals bond strength can appear as rotational energy in the diatomic.

The binding energies of the rare-gas I_2 series for the ground state and excited complexes were determined[7] by using the anharmonicity of the I_2 *B*-state to bracket the binding energy in the excited state, then adding the observed band shift to obtain the ground state binding energy. Morse potential parameters were also reported as determined from van der Waals vibrational progressions noted in the excitation spectra. It is interesting to note that even though the complex Ar-$I_2(X,v''=1)$ is energetically stable, that is, the vibrational frequency (213.3 cm^{-1}) is exceeded by the Ar-$I_2(X)$ bond strength (~235 cm^{-1}), evidence of the "hot-band" complex was not observed.[6]

The theoretical efforts of Beswick, *et al.*,[8-12] have attempted to simulate the results of the Levy experiments. The model first advanced involved the collinear vibrational predissociation of the van der Waals complex *X-BC*[8,9] where *BC* is a diatomic molecule and *X* is a rare-gas atom. The *BC* diatomic bond was characterized by either a harmonic or Morse potential. The van der Waals bond was described by a Morse function. In developing the vibrational predissociation rate model, the coupling of discrete states of the zero-order Hamiltonian ($H_{BC} + H_{X,BC}$) to other discrete states was neglected. Intercontinuum coupling, which

effects the final vibrational energy distribution in the diatomic fragment, was found to be significant only between states in which the change in vibrational quantum number was ±1. However, the discrete-continuum coupling, which, through Golden Rule arguments, gives rise to the vibrational predissociation rate of the initially prepared complex, is considered for all energy-allowed ("open") channels i.e. Δv=-1, -2, -3,...,etc. The result for the collinear case in which the *BC* potential is assumed harmonic, is a closed analytical expression for the vibrational predissociation rate in terms of potential parameters, diatomic and van der Waals vibrational quantum numbers. The rate expression establishes the "energy-gap" law: $\Gamma_{v,l} \propto \exp\left[-(D^{\frac{1}{2}}_{X,BC}/\omega_{XB})\omega^{\frac{1}{2}}_{BC}\right]$, with Γ being the vibrational predissociation half-width, D_{XB} the van der Waals dissociation energy and ω_{BC}, ω_{XB} the diatomic and van der Waals stretching frequencies respectively. Also made evident was the effect of the reduced mass ($\Gamma_{v,l} \propto -\mu^{\frac{1}{2}}_{X,BC}$), dependence on diatomic stretch quantum number v ($\Gamma_{v,l} \propto v$), and van der Waals mode quantum number l ($\Gamma_{v,l} \propto \exp[(N-l-1)^2]$) where N is the number of bound levels for the van der Waals mode. The use of a Morse potential for describing the *BC* diatomic led to the observation that the dependence of the rate upon *BC* vibrational quantum number is superlinear ($\Gamma_{v,l} \approx Av + Bv^2$). Although the absolute rates calculated are not in good agreement with the observed rates for He-I_2, the model is in qualitative agreement regarding the propensity rule Δv=-1 and the superlinear dependence of rate on the vibrational quantum number.

The model for vibrational predissociation was improved by considering the *T*-shaped molecule with the rare-gas atom restricted to move perpendicular to the diatomic axis.[10] The interaction between the

rare-gas atom and the diatomic was represented by a sum of Morse potentials. Unlike the collinear case, this model did not result in an analytical solution; rather, the close-coupled equations were solved numerically. It was found that the vibrational predissociation rate Γ for T-shaped He-I_2 (B) was approximately an order of magnitude smaller than the calculated rate for the collinear molecule. The inclusion of anharmonicity of the I_2 bond[11] in the T-shaped He-I_2 model led to a superlinear dependence of Γ upon v in good agreement with experimental results. Finally, the influence of the rotational degrees of degrees of freedom on the vibrational predissociation rate was investigated.[12] For the initially prepared He-I_2 (B,v'=25) complex with $J_{complex}$=0, the final rotational distribution of the I_2 fragment has the maximum occurring at J_{I_2}=2 ($E_{rot} \simeq 0.18$ cm^{-1}). The calculated vibrational predisociation rate is only a factor of 2-3 smaller than that of the perpendicular model ignoring the effect of rotation. Since the fraction of available energy going into rotation was found to be very small compared to the final translational energy of the fragments, it was concluded that vibrational predissociation in He-I_2 is essentially a pure $V \rightarrow T$ process.

Ewing, in addressing the role of vibrational predissociation of van der Waals molecules in vibrational relaxation processes, applied the Golden Rule to determine $V \rightarrow T$ lifetimes of excited complexes.[13] From the calculated vibrational predissociation rates, the equilibrium constants for several van der Waals species were computed. The study led to the conclusion that van der Waals molecules play a significant role in vibrational relaxation processes at very low temperatures, e.g. T on the order of half the well depth ($T \approx E/2k$). In examining the dependence of the lifetime upon the molecular parameters, an insightful correlation was

recognized. It was observed that a logarithmic plot of $V \rightarrow T$ lifetimes vs. the quantity $(2\mu\Delta E)^{1/2}/\alpha\hbar$ where μ is the reduced mass of the complex, ΔE the kinetic energy of the fragments, and α is the Morse range parameter, yields very nearly a straight line for the species considered.[14] A simple explanation for the correlation was offered. The quantity $p=(2\mu\Delta E)^{1/2}$ corresponds to the relative translational momentum of the fragments. In the Golden Rule expression, the final state function will be modulated by the deBroglie plane wave with corresponding wavelength given by $\lambda=h/p$. The initial van der Waals vibrational wave function resembles a Gaussian along the van der Waals coordinate. The lifetime of the complex is then governed by the overlap of the final state plane wave with the initial Gaussian wave function through the coupling term. Clearly, the overlap of initial and final state functions will be increased as the relative translational momentum, the "momentum-gap" is reduced, hence decreasing the lifetime. The correlation serves as a guide for estimating the lifetime of vibrationally excited van der Waals Molecules, provided the Morse range parameter α and the internal energy distribution of the fragments is known reasonably well.

In a previous communication,[15] the observation of the metastable vibrationally excited van der Waals molecule Ne-Cl_2 ($X,v''=1$) was reported. The present paper concerns itself with the details of the spectroscopic studies performed upon the Ne-Cl_2 molecule at ~0.2 cm^{-1} resolution. Section II of the paper describes in detail the pulsed molecular beam apparatus employed in the spectroscopic measurements of the Ne-Cl_2 molecule. Spectra originating from the ground and vibrationally excited states of Ne-Cl_2 are shown in Section III. The results of fitting the spectra by a non-linear least squares to an asymmetric top model in

order to determine band origins and structures are also given in Section III. The significance of the structure and observed band origins for the complex is discussed in Section IV. Also included in Section IV are estimates of the vibrational predissociation lifetimes for the Ne-Cl_2 (X,v''=1) and Ne-Cl_2 (B,v') complexes as determined by the "energy-gap" collinear harmonic model and the "momentum-gap" correlation diagram. The paper concludes with suggestions for further spectroscopic investigations designed to extract accurate lifetime, detailed structural and dynamical information of the Ne-Cl_2 molecule.

II. Experimental

The pulsed molecular beam apparatus employed in these measurements is diagrammed in Figure 1. The main chamber is constructed of 3/4" thickness aluminum plate welded to form a cube approximately 45 cm on edge. The pulsed nozzle assembly is mounted on a *xyz*-translation stage such that the molecular beam is directed towards the pump. A pair of fixed, vertically mounted light baffles defines the laser beam path through the apparatus. Total and dispersed fluorescence collection optics are mounted mutually perpendicular to both the laser and molecular beams, and may be translated along the molecular beam axis.

During operation, the apparatus is maintained at pressures below 10^{-4} torr by a Varian HS16 diffusion pump capable of delivering a pumping speed of 10,000 l/s. The diffusion pump is backed by a Leybold-Heraeus WS-160 Roots blower in series with a Heraeus-Engelhard DK-20 mechanical pump. An interlock-activated pneumatic 16-inch gate valve protects the diffusion pump in the event of a chamber overpressure condition. The inclusion of a valved roughing port utilizing the forepump permits rapid access to the main chamber. Under typical operating conditions the average gas throughput of the system is about 0.5 torr l/s, below the ultimate system throughput capability of 1 torr l/s.

A solenoid-actuated impact valve is used to produce the pulsed supersonic beams containing van der Waals molecules. The pulsed beam source is similar in design to a modified commerical solenoid valve (Peter Paul Electronics #H22G7DCM) used in the Rice group at the University of Chicago.[16] A 1ms current pulse, when applied to the solenoid coil, accelerates the soft iron plunger which moves freely until it impacts the lip of the seating pin thus opening the valve. High pressure gas flows past

Figure 1. Diagram of pulsed nozzle apparatus.

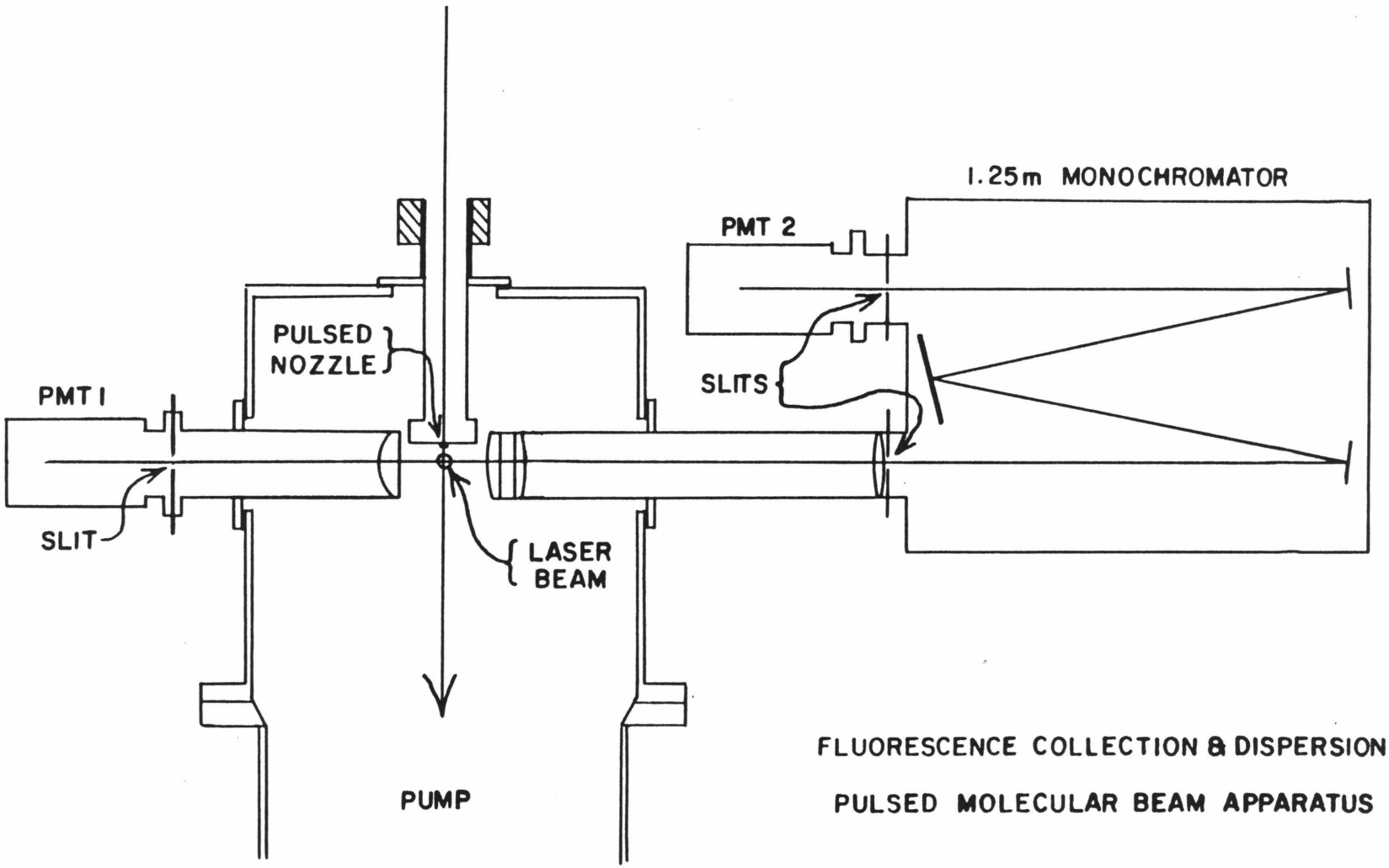

FLUORESCENCE COLLECTION & DISPERSION

PULSED MOLECULAR BEAM APPARATUS

the valve seat and through a 400 micron electron microscope aperture into the vacuum apparatus to form the molecular beam. The head of the seating pin is in direct contact with the closing spring, therefore the valve remains open for only a short time. Careful adjustment of mechanical and electrical parameters permits formation of pulsed beams with durations of less than 300 μs.

An excimer-pumped dye laser (Lambda-Physik FL 2002) provides the tunable excitation radiation for these measurements. Pumped by a XeCl excimer laser (Lumonics 861-S) delivering approximately 80mJ of 308 nm radiation per pulse, the dye laser produces ~8mJ pulses from Coumarin 503 in the 490-540 nm region. The frequency bandwidth of the laser varies from 0.10 to 0.30 cm^{-1} in this region, depending on grating order and operating wavelength of the laser. The unfocussed dye laser beam is directed by means of kinematically-mounted mirrors through the light baffles on the vacuum apparatus. The baffles are equipped with Brewster angle mounted Supracil 2 windows and knife-edged apertures designed to minimize admission of stray light without incurring excessive refractive scattering of the dye laser beam.

The total fluorescence collection optical system consists of a 75mm diameter aspheric lens (f/0.7), which projects the fluorescence region image onto defining slits approximately 35 cm from the interaction region. A cutoff filter (Schott OG-515, etc.) is used to remove scattered laser light since the bulk of the Cl_2 molecular fluorescence is expected to be red-shifted 30 nm or more on the basis of published Franck-Condon factors.[17] The apparatus is also equipped with fluorescence collection optics designed to closely match the etendue of a 1.26m 1800mm^{-1} grating spectrometer (Spex 1269). A condenser (f/1.2)

magnifies the fluorescence image by a factor of six onto the spectrometer slits. A field lens just in front of the slit fills the grating with fluorescence radiation insuring maximum spectrometer performance.

The data acquisition system for the pulsed molecular beam apparatus is depicted in Figure 2. The system is controlled by an IBM-PC microcomputer through a commercially available interface card (Tecmar Labmaster). The microcomputer operates in an interrupt-driven mode under the PC-FORTH system (Laboratory Microsystems, Inc.). A typical acquisition cycle timing sequence is also shown in Figure 2. The computer first triggers the pulsed valve driver which generates the current pulse to the solenoid coil. After 1-2 ms (depending upon the characteristic delay in valve opening) the microcomputer then triggers the MCSA. Approximately 15 μs after initiating the MCSA averaging cycle, the excimer laser is triggered. The transient fluorescence signal, obtained from a cooled photomultiplier tube (RCA 31034), is digitized and summed into the MCSA memory. This sequence is typically repeated ten times for each laser freqency point. The microcomputer then extracts the fluorescence intensity from the proper MCSA time channels, updates the display and steps the dye laser grating to the next frequency point. This process is continued until the scan is completed. The microcomputer writes the scan parameters and spectral data onto magnetic disk for future analysis.

The helium, neon, and chlorine gases for the mixtures were used as supplied (Matheson) without further purification. The mixtures were prepared in a Monel metal cylinder by addition of the appropriate partial pressures of the component gases. The cylinder was agitated thoroughly before use to insure homogeniety of the gas mixture.

Figure 2. Block diagram of the data acquisition system. The timing sequence is shown on the lower portion of the figure.

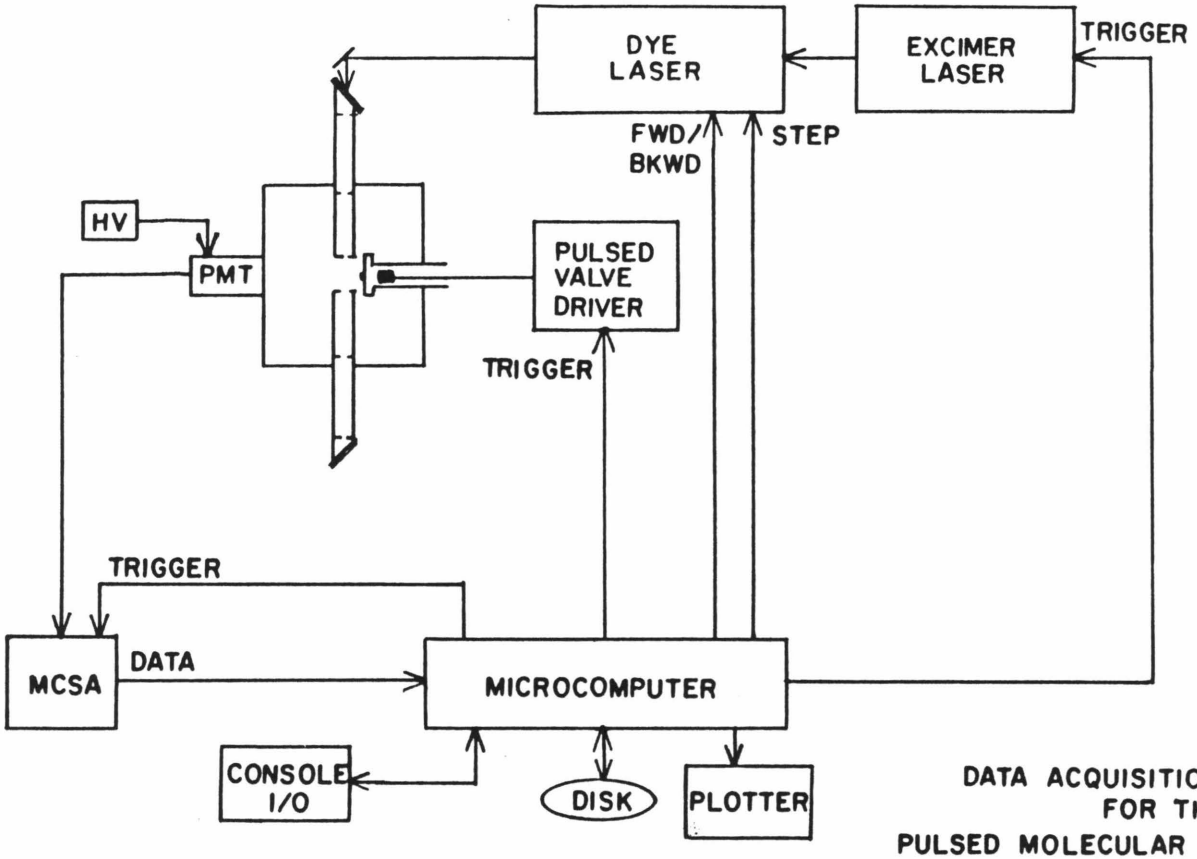

DATA ACQUISITION SYSTEM
FOR THE
PULSED MOLECULAR BEAM APPARATUS

TIMING SEQUENCE

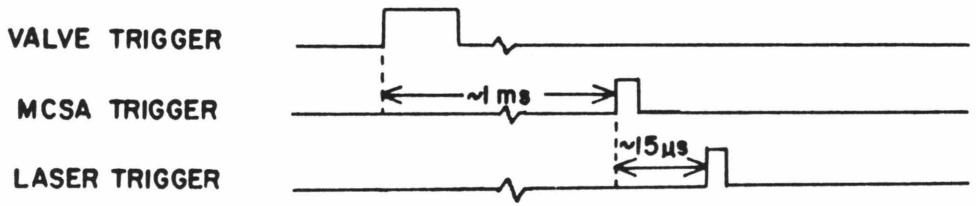

III. Results

A. Spectroscopy of Ne-Cl_2 ($X^1\Sigma^+$,v''=0)

The laser-induced fluorescence excitation spectrum of a pulsed molecular beam containing natural isotopic abundance molecular chlorine, neon, and helium in the vicinity of the $B^3\Pi_{(0^+)} - X^1\Sigma^+$ (11-0) vibronic transitions is shown in Figure 3. The bands with easily discerned rotational structure are due to, in order of increasing intensity, the $^{37}Cl_2$, $^{35}Cl^{37}Cl$, and $^{35}Cl_2$ isotopic variants of molecular chlorine. It should be noted that the $^{35}Cl_2$ bandhead was of sufficient intensity to exceed the input dynamic range of the MCSA and, based on isotopic abundances, the actual intensity of this feature should be approximately 1000 signal units greater than what appears in Figure 3. Still clearly visible, however, are the effects of nuclear spin statistics upon the intensities of the rovibronic transitions for the homonuclear ($^{35}Cl_2$ and $^{37}Cl_2$) versus the heteronuclear ($^{35}Cl^{37}Cl$) species. Both isotopes of chlorine are fermions with nuclear spin I=3/2 which leads to a 5:3 alternation of statistical weights for odd and even J levels of the homonuclear diatomic species. The effective rotational temperature and laser bandwidth (assumed to have a Gaussian frequency dispersion) were determined by modeling the (11-0) band of $^{35}Cl_2$ with a non-linear least squares fitting program. Using the rotational constants $B_{v'=11}$ = 0.12616 cm^{-1} and $B_{v'=0}$ = 0.24327 cm^{-1} as reported by Coxon,[18] the fit yields T_{rot} = 4.0K and $\Delta\nu_{laser}$ = 0.20 cm^{-1}.

The spectroscopic features occuring approximately 5.3 cm^{-1} to higher energy of the $^{35}Cl_2$ and $^{35}Cl^{37}Cl$ bandheads in Figure 3 are observed only in molecular beams formed from mixtures containing Ne as well as Cl_2 and He. The integrated intensity of the feature to the blue of the $^{35}Cl_2$ (10-0) vibronic band, normalized to the Cl_2 integrated intensity, as a

Figure 3. Laser-induced fluorescence spectrum in the vicinity of the $B-X$ (11-0) vibronic band for Cl_2. Spectrum was obtained by expanding .5% Cl_2 : 25% Ne : Bal. He at 150 psi through a 400 μ nozzle.

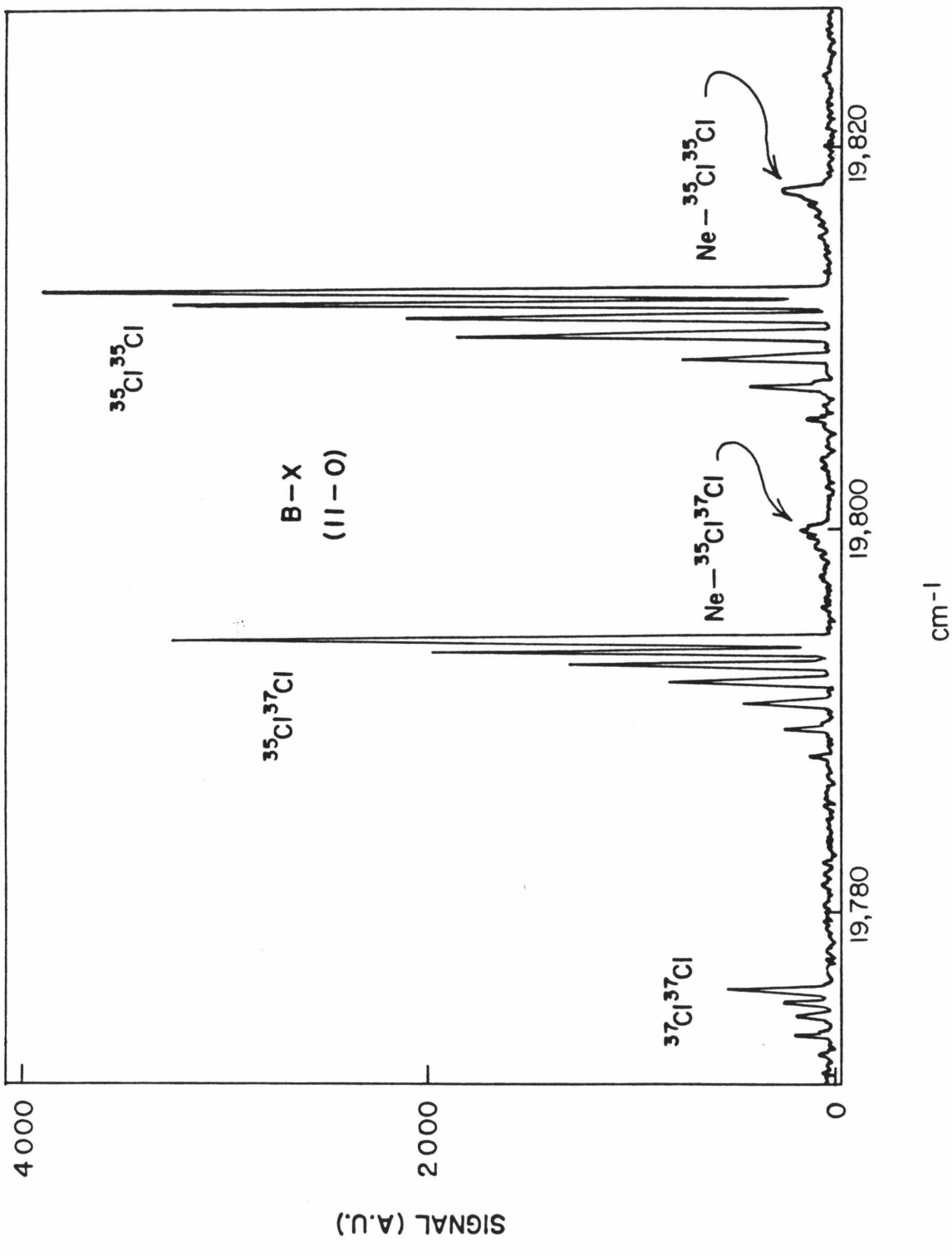
SIGNAL (A.U.)
4000
2000
0
19,780
19,800
19,820
cm-1
$^{37}Cl^{37}Cl$
$^{35}Cl^{37}Cl$
$^{35}Cl^{35}Cl$
B–X
(11–0)
Ne–$^{35}Cl^{37}Cl$
Ne–$^{35}Cl^{35}Cl$

function of source pressure is plotted in Figure 4. Since $I_{Cl_2} \propto P$ and the slope of the plot yields $I_{NeCl_2} / I_{Cl_2} \propto P^{1.4}$, the pressure dependence for Ne-Cl_2 formation is $I_{NeCl_2} \propto P^{\sim 2.4}$. A cubic pressure dependence might be expected since the simplest scheme for formation of Ne-Cl_2 involves the three-body collision:

$$Ne + Cl_2 + M \rightarrow Ne{-}Cl_2 + M$$

where M removes the heat of formation of the van der Waals complex as relative kinetic energy. The actual kinetics of formation of Ne-Cl_2 in a comparatively rich expansion mixture are certainly more complicated than just the above reaction. In an expansion containing 25% Ne, a considerable amount of the van der Waals dimer Ne_2 would be expected to form. Then a two-body collision such as:

$$Cl_2 + Ne_2 \rightarrow Ne{-}Cl_2 + Ne$$

which is a far more likely process than three-body collisions in an expanding beam, can lead to formation of Ne-Cl_2. The chemistry is further complicated by reactions which deplete Ne-Cl_2 in the beam such as:

$$Ne{-}Cl_2 + Cl_2 \rightarrow (Cl_2)_2 + Ne\ .$$

Therefore, the value of the pressure exponents does not always provide conclusive information concerning the identity of a van der Waals species.[19]

Excitation spectra were also obtained in the vicinity of the (6-0) through (16-0) vibronic origins of the $^{35}Cl_2$ $B{-}X$ system. Bands of similar relative intensity to the feature to the blue of the (11-0) bandhead were observed at nearly constant frequency shifts from each of the uncom-

Figure 4. Pressure dependence of integrated intensity of Ne-Cl_2 band.

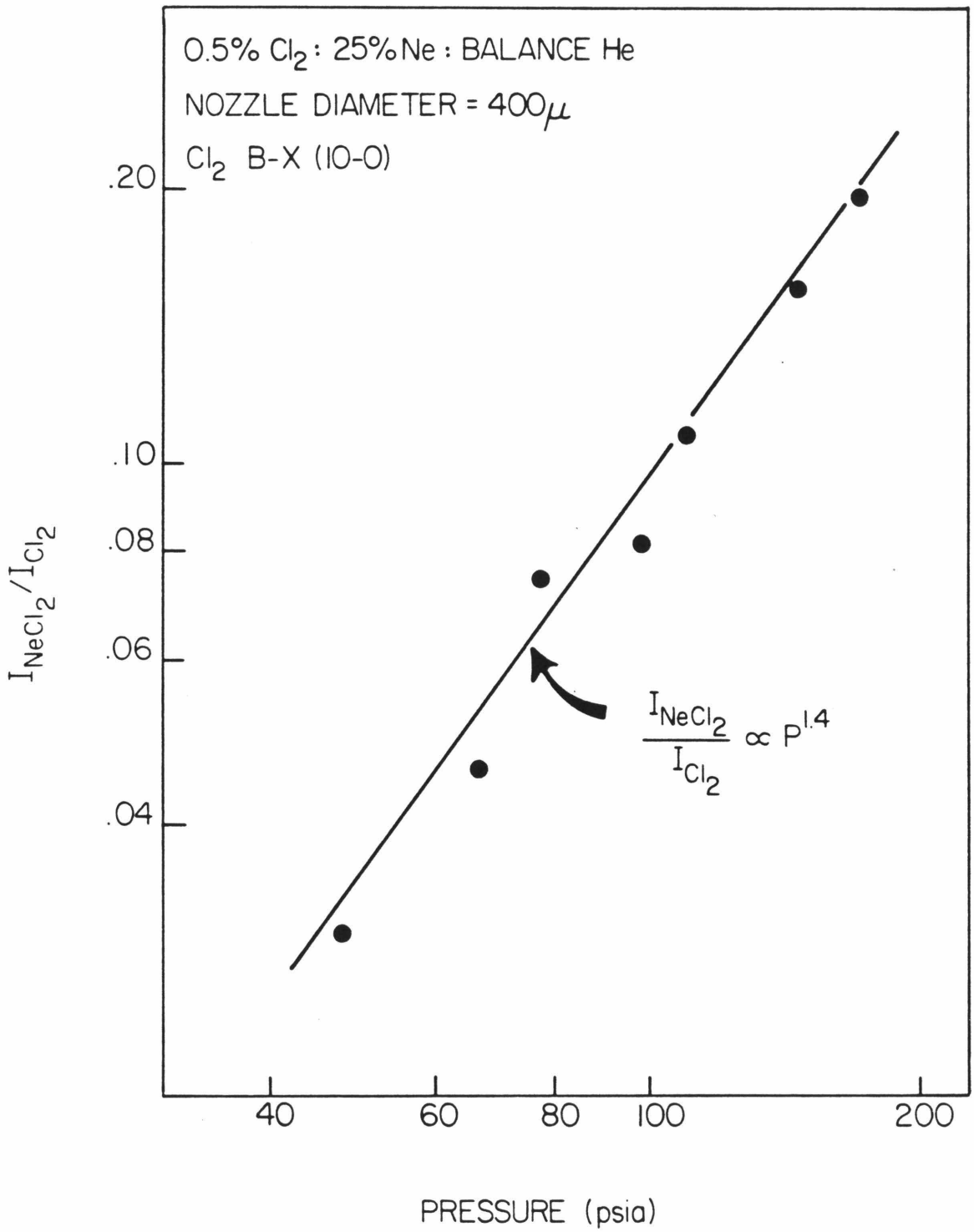
0.5% Cl_2 : 25% Ne : BALANCE He
NOZZLE DIAMETER = 400μ
Cl_2 B-X (10-0)
.20
.10
.08
.06
.04
I_{NeCl_2}/I_{Cl_2}
$\frac{I_{NeCl_2}}{I_{Cl_2}} \propto P^{1.4}$
40
60
80
100
200
PRESSURE (psia)

plexed $^{35}Cl_2$ band origins. The positions and shifts of the origins of the bands due to the complex relative to the $^{35}Cl_2$ ($v'-0$) band origins are given in Table I. The positions of the band origins for the van der Waals bands were determined by fitting an asymmetric top bandshape to the experimental data by the non-linear least squares program described more fully in Section C.

B. Spectroscopy of Ne-Cl_2 ($X^1\Sigma^+$,v''=1)

The laser excited fluorescence spectrum of the $B-X$ (10-1) hot-band for $^{35}Cl_2$ is shown in Figure 5. The observation of the spectrum arising from vibrationally-excited chlorine molecules in a supersonic molecular beam is not suprising since high-frequency vibrations do not relax rapidly under the conditions of expansion. In addition, the Franck-Condon factors[17] for the hot-band transitions are an order of magnitude greater than the transitions to the corresponding levels from the ($v''=0$) level. The measured intensities of the hot-bands relative to bands arising from $Cl_2(v''=0)$ indicates an effective vibrational temperature of 200-250K in the beam. The rotational temperature of $^{35}Cl_2$ ($v''=1$) was determined to be 3.7K by fitting the (10-1) spectrum using the literature constants[18] $B_{v''=10} = 0.13018\ cm^{-1}$ and $B_{v''=1} = 0.24165\ cm^{-1}$.

The observation of the feature appearing approximately 5.0 cm^{-1} to higher energy of the (10-1) bandhead in Figure 5 *is* rather unexpected. The integrated intensity of this feature has been measured as a function of stagnation pressure and is found to vary as $I \propto P^{\sim 2.5}$. Similar bands are found to occur near the (8-1) through the (12-1) hot-bands of Cl_2, the frequency shifts of which are also given in Table I. The energy of vibration for $^{35}Cl_2(X\ ^1\Sigma_g^+)$ is ~560 cm^{-1} while the van der Waals bond strength for

Table I.

Band shifts for the Ne-Cl_2 van der Waals molecule.

Band	ν_{00} ($^{35}Cl_2$)[a]	ν_{00} (Ne–$^{35}Cl_2$)[b]	Shift
6-0	18993.788	18999.14(18)*	5.35
7-0	19179.307	19185.01(13)	5.70
8-0	19353.976	19359.57(16)	5.59
9-0	19517.746	19523.39(14)	5.65
10-0	19670.509	19676.35(21)	5.84
11-0	19812.366	19817.75(18)	5.38
12-0	19943.390	19948.95(13)	5.56
13-0	20063.670	20069.54(15)	5.87
14-0	20173.447	20180.49(26)	7.05
15-0	20273.263	20280.65(17)	7.38
8-1	18799.66	18805.34(18)	5.67
9-1	18969.43	18969.10(19)	5.67
10-1	19116.210	19121.40(12)	5.19
11-1	19258.051	19263.58(14)	5.53
12-1	19389.036	19394.76(07)	5.72

[a] Band origins reported by Coxon in Ref. 18.

[b] This work.

* Uncertainty taken as laser bandwidth.

Figure 5. Spectrum showing pressure dependence of $Ne\text{-}Cl_2$ (10-1) band.

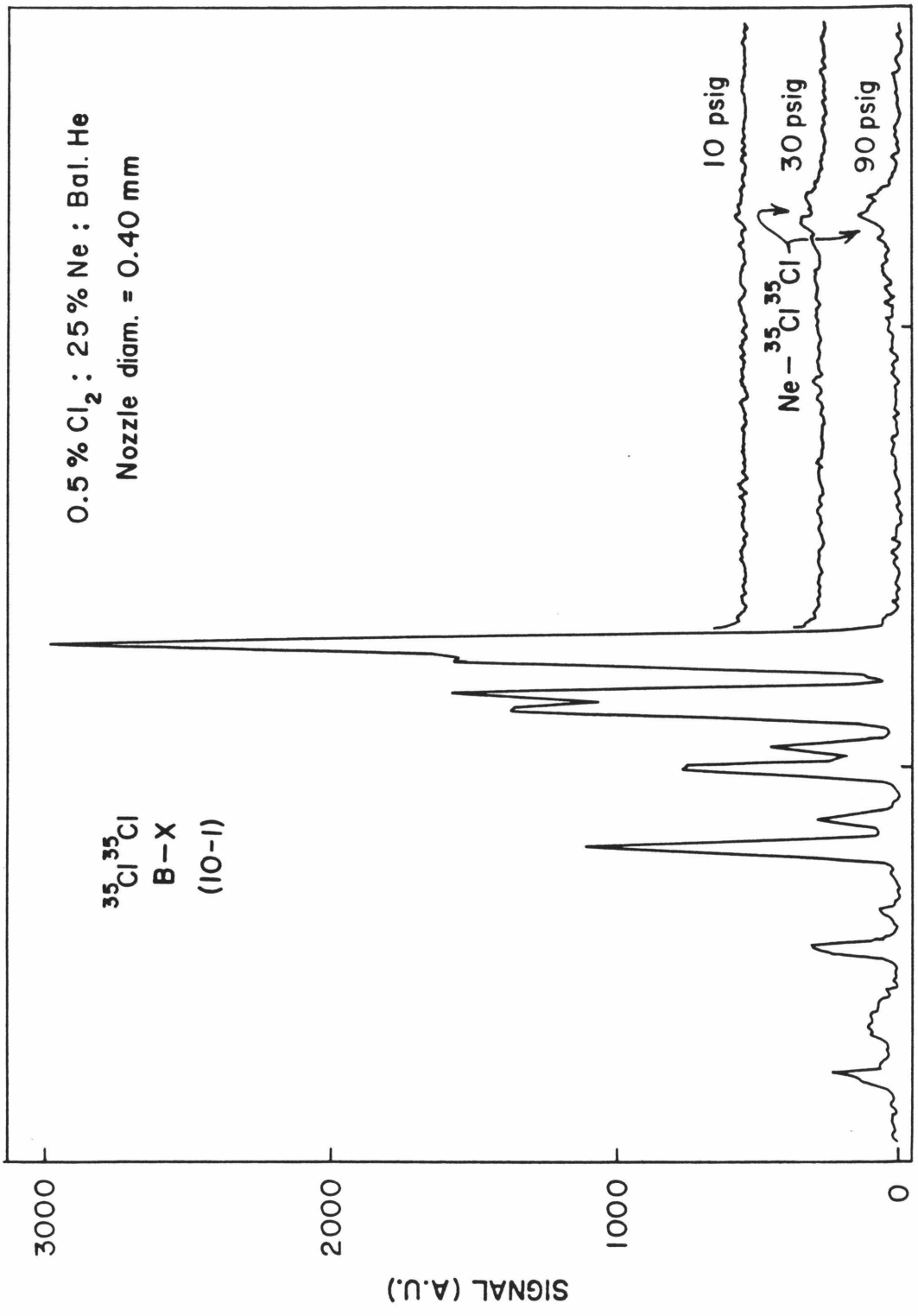
0.5 % Cl_2 : 25 % Ne : Bal. He
Nozzle diam. = 0.40 mm
$^{35}Cl^{35}Cl$
B – X
(10-1)
10 psig
30 psig
90 psig
Ne – $^{35}Cl^{35}Cl$
SIGNAL (A.U.)
3000
2000
1000
0
19,115
19,120
cm^{-1}

Ne-Cl_2 should be less than 75 cm^{-1} (as determined for Ne-I_2 (X)),[7]. In consideration of these energies the observed species, Ne-Cl_2 ($X\ ^1\Sigma^+, v''=1$), *is a metastable vibrationally- excited van der Waals molecule.*

Assuming typical molecular beam velocity ($v=10^5$ cm/s) and a 1 cm nozzle to laser interaction region distance provides a **lower** bound for the lifetime of this "hot-band" complex $\tau = 10^{-5}$ s. The direct measurement of the lifetime of the complex has been attempted by increasing the flight path from the nozzle to laser interaction region by about 1 cm. Taking into account the the diminishing number density of the complex from the $1/r^2$ beam intensity decrease, no pronounced decay of the complex was observed.

C. Structure of the Ne-Cl_2 van der Waals Molecule

With more extensive signal averaging, evidence of rotational structure in the fluorescence bands due to Ne-Cl_2 became apparent (see Figure 6). Although the laser bandwidth (~0.2 cm^{-1}) prohibits observation of the fully resolved rovibronic spectrum, the band profiles obtained do permit some structural investigation by a non-linear least squares fitting program. The program adjusts the molecular structural parameters in order to fit the modeled band shape to the observed spectrum. The model includes the effects of nuclear spin statistics as well as molecular parameters corresponding to the band origin and the effective rotational temperature. Values for the parameters characterizing the dye laser bandwidth and frequency offset are established first by fitting the uncomplexed chlorine band using the literature values for the rotational constants and band origin for the vibronic transition of interest. The rotational temperature of Cl_2 is also determined in this preliminary fitting.

Figure 6. Averaged spectrum of Ne-Cl_2 (11-0) band. Note the evidence of rotational structure in the red-shaded portion of the band.

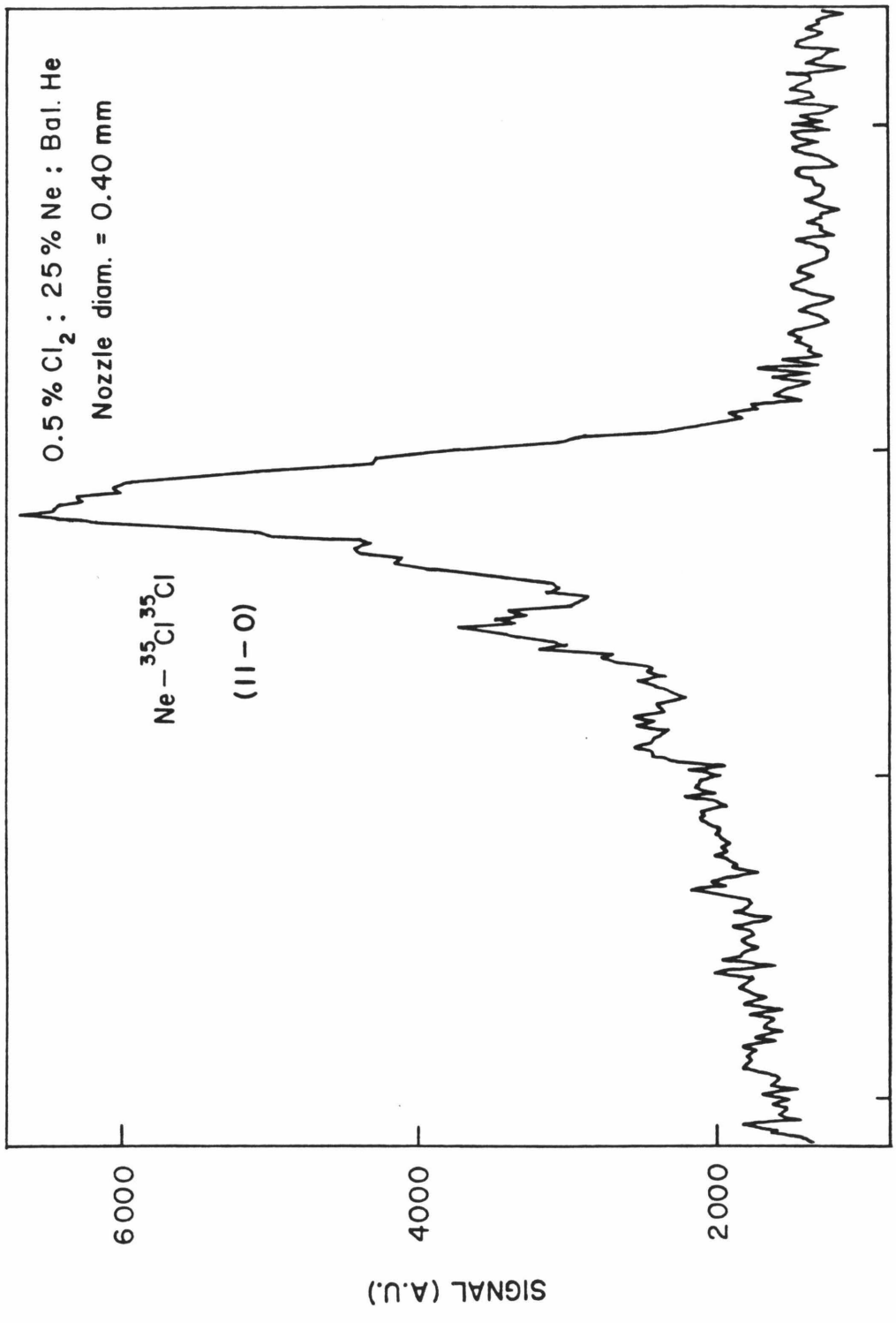
0.5 % Cl_2 : 25 % Ne : Bal. He
Nozzle diam. = 0.40 mm
$Ne-{}^{35}Cl\,{}^{35}Cl$
(11 – 0)
SIGNAL (A.U.)
6000
4000
2000
19,814
19,816
19,818
19,820
cm^{-1}

The computed band shapes for Ne-Cl_2 near the (11-0) and (11-1) transitions are illustrated in Figures 7 and 8. The points represent the observed spectra while the solid curves describe the best fit to the data. It should be noted that attempts to fit the spectra with a collinear structure failed to qualitatively describe the observed band shape, in particular the structure on the red-shaded portion of the band, over a large variation in Ne-Cl_2 separation. For the band shapes shown in Figures 7 and 8, the complex was assumed to be a *T*-shaped molecule with the Cl_2 internuclear separation essentially unperturbed by the presence of the Ne atom. The dashed line corresponds to the computed band shape obtained for the Ne-Cl atom-atom separation taken to be the same as that determined for Ne-Ar by crossed molecular beam scattering measurements.[20] The best fit structure indicates that the potential minimum for ground state Ne-Cl_2 occurs at 3.61±.08 Å.

Figure 7. Model fits to the observed Ne-Cl_2 (11-0) band (points).

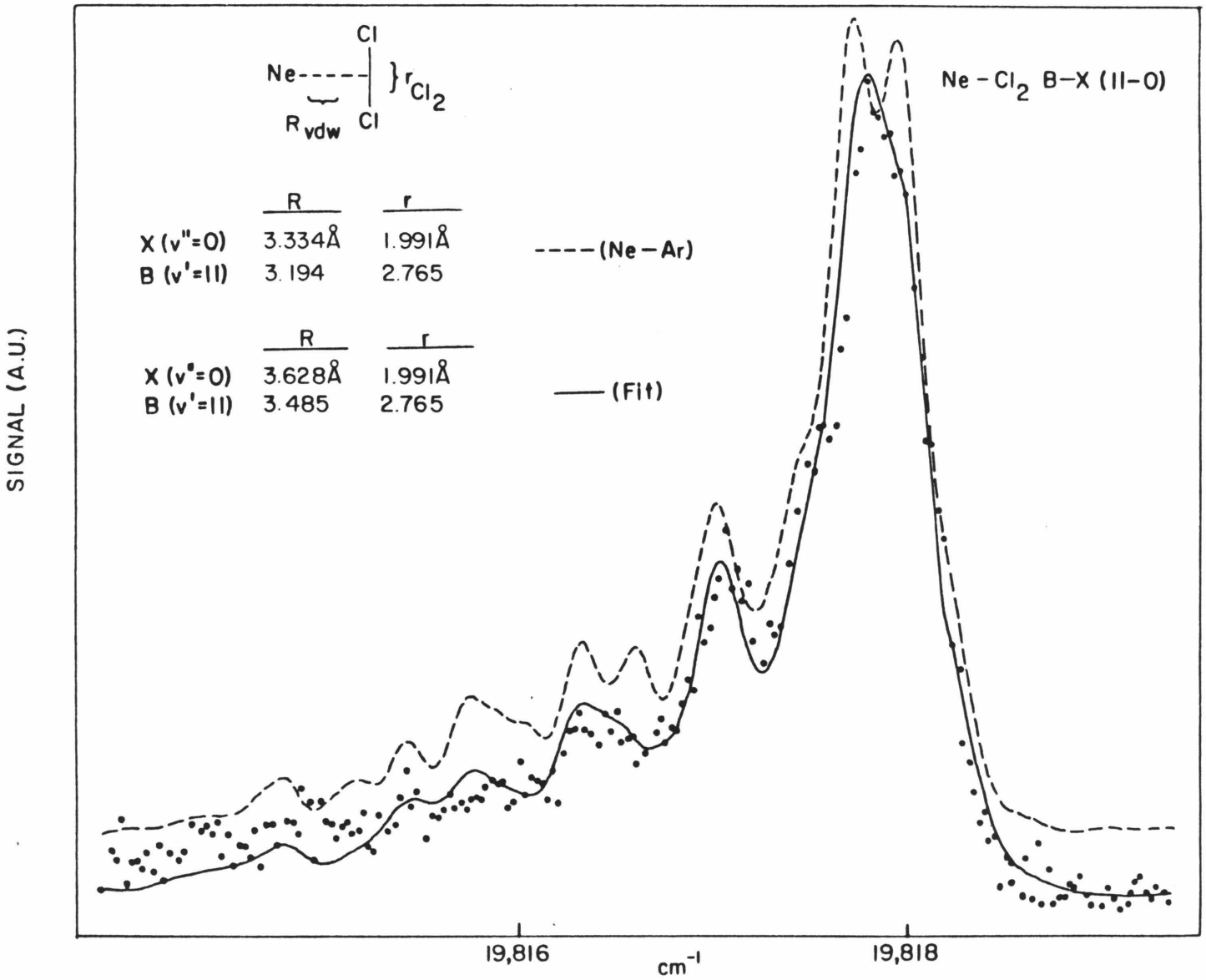
Cl
Ne
Cl
r_{Cl_2}
R_{vdw}
Ne – Cl_2 B–X (11–0)
R r
X (v"=0) 3.334Å 1.991Å
B (v'=11) 3.194 2.765
----(Ne–Ar)
R r
X (v"=0) 3.628Å 1.991Å
B (v'=11) 3.485 2.765
——(Fit)
SIGNAL (A.U.)
19,816
19,818
cm⁻¹

Figure 8. Model fits to the observed Ne-Cl_2 (11-1) band (points).

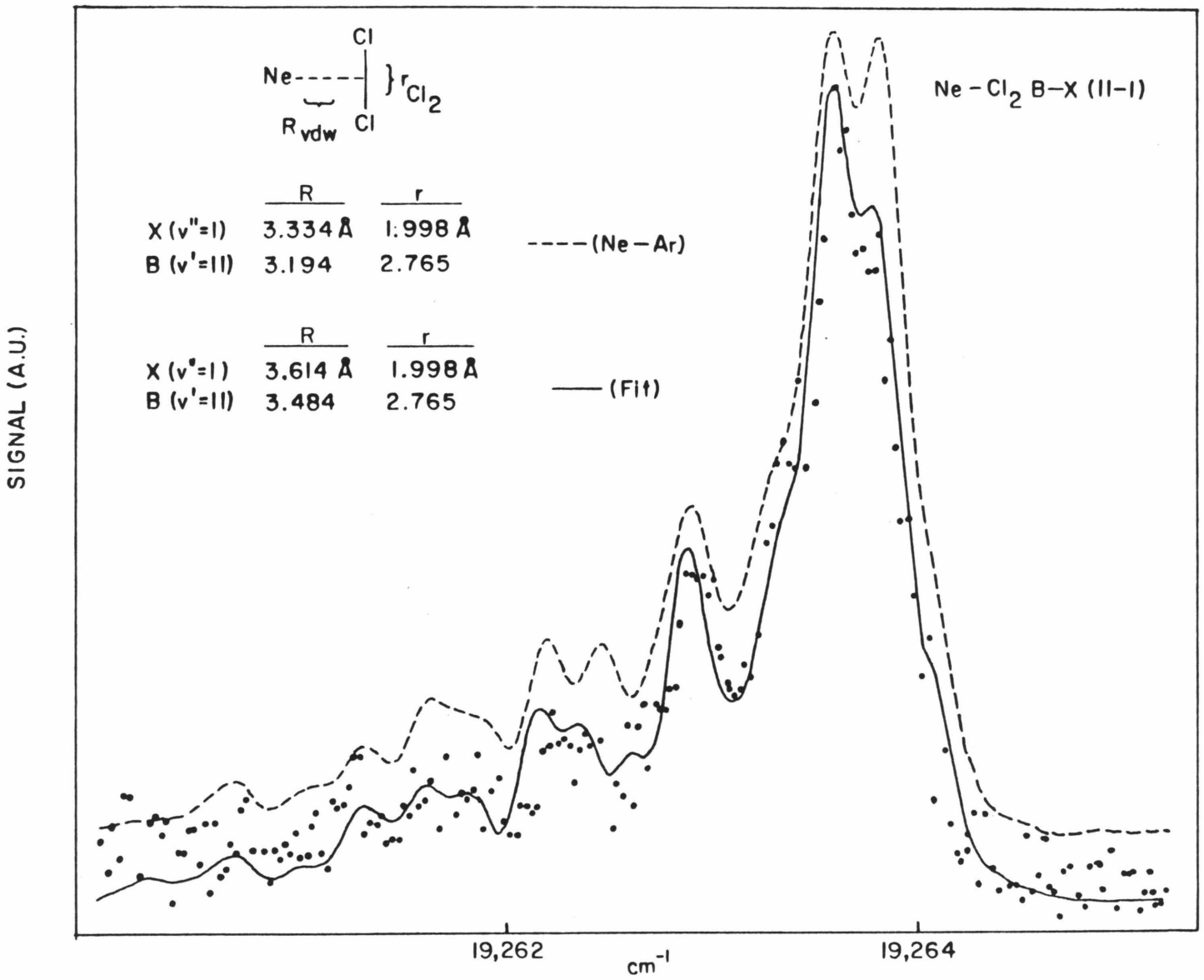
Cl
Ne
Cl
R_{vdw}
r_{Cl_2}
R r
X (v"=1) 3.334 Å 1.998 Å
B (v'=11) 3.194 2.765
R r
X (v"=1) 3.614 Å 1.998 Å
B (v'=11) 3.484 2.765
----(Ne-Ar)
——(Fit)
Ne - Cl_2 B-X (11-1)
SIGNAL (A.U.)
19,262
19,264
cm^{-1}

IV. Discussion

The absolute value for the frequency shift of the bands due to a van der Waals molecule relative to the corresponding free constituent provides only a measure of the comparative binding energy in the upper and lower states. A series of measurements, as reported in Table I, originating from a common ground level does provide information concerning the nature of the van der Waals interaction in the vertically excited state. The band shifts of the $B-X$ $(v'-0)$ transitions for Ne-Cl_2 are plotted in Figure 9. In contrast to the I_2 van der Waals molecules,[5] the band shift is not a smooth, monotonically increasing function of the upper vibrational quantum number. Rather, there is a considerable ($\sim$1 cm^{-1}) break in the band shift between the (13-0) and (14-0) transitions. Presumably this abrupt increase in destabilization of the complex at higher vibrational excitation is due to a perturbation of the van der Waals potential surface arising from the repulsive limb of the $A^3\Pi_{1_u}$ state of Cl_2. The $A^3\Pi_{1_u}$ state, which has been predicted to provide the predissociative channel for the B-X system of Cl_2 above the (v'=12) level,[21] correlates to ground state chlorine atoms. The predissociation rate was found to have a $J'(J'+1)$ dependence,[22] indicating a strong heterogeneous ($\Delta\Omega=\pm1$) interaction between the $B^3\Pi_{(0_u^+)}$ state and the repulsive wall of the $A^3\Pi_{1_u}$ state. The effect of this perturbation became evident in our Cl_2 spectra for ($v'\geq13$) where the P(1) line is the strongest feature rather than the line corresponding to the blended R(0) and R(1) transitions, which dominates the spectra for $v'\leq12$. Since above the (v'=12) electronic predissociation threshold, the quantum yield of fluorescence drops by several orders of magnitude, the quality of data suffers in this interesting region. Unfortunately, data obtained with the present resolution does not permit

Figure 9. Plot of band shift vs. *B*-state vibrational quantum number for Ne-Cl_2.

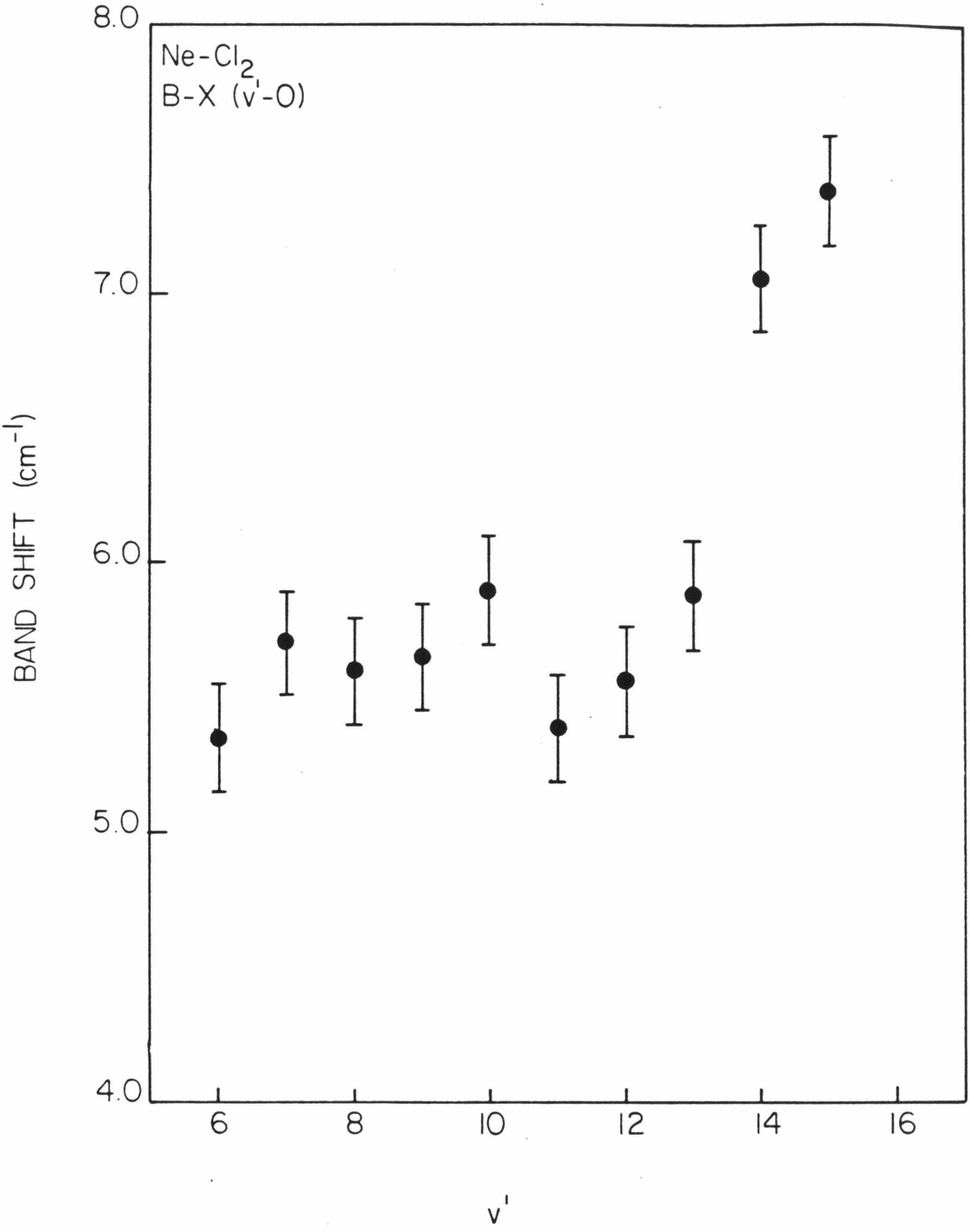
8.0
7.0
6.0
5.0
4.0
Ne-Cl2
B-X (v'-0)
BAND SHIFT (cm-1)
6
8
10
12
14
16
v'

further discussion of the influence of the perturbing state on the van der Waals interaction nor of the effect that a van der Waals partner may have on such a perturbation.

The structure of the Ne-Cl_2 molecule, like He-I_2, [2] is *T*-shaped as indicated from fits to the band profiles shown in Figures 7 and 8. The *T*-shaped structure is what would be expected if the intermolecular interaction is described by a pairwise additive potential. As pointed out by Levy,[5] the donor-acceptor model[23] would predict a linear ground state structure since the acceptor orbital would be the σ_u* orbital on the halogen. Upon excitation the π_g* orbital becomes the lowest unoccupied orbital, indicating a bent structure. There is no indication of a large geometry change in the spectra such as a van der Waals vibrational progression. The relatively small frequency shift observed for the complex implies that there is little difference between the ground and excited state potentials.

A first guess for the Ne-Cl_2 pair-wise model potential might be constructed by replacing the Cl atoms with Ar atoms and using the Ne-Ar parameters (r_{min}= 3.48 Å, ε = 52 cm^{-1}).[20] Note that the Ne-Cl_2 separation calculated by this model (3.33A) is approximately 0.3Å shorter than the fit indicates. Also, the well-depth based on additivity of the Ne-Ar potentials (~104 cm^{-1}) is considerably larger than that for Ne-I_2 (70 cm^{-1}). Intuitively one might expect a shallower well for Ne-Cl_2 than for Ne-I_2 according to the relative polarizabilities of Cl_2 and I_2. The Ne-Cl_2 distance, as determined from the fit (3.61±.08Å), is only approximately 0.1Å shorter than the estimated collinear potential minimum reported by Secrest and Eastes,[24] obtained by averaging the Cl_2-Cl_2 and Ne-Ne intermolecular potentials.[25]

Table II presents a comparative listing of estimated vibrational

Table II.

$Ne\text{-}Cl_2(v) \rightarrow Ne + Cl_2(v-1)$

Estimated Vibrational Predissociation Lifetimes and Linewidths

Cl_2 Initial State	Momentum-Gap			Energy-Gap	
	$(2\mu\Delta E)^{1/2}/\alpha\hbar$	τ (s)	$\Gamma(cm^{-1})$	τ (s)	$\Gamma_{v0}(cm^{-1})$
$(X,v''=1)$	16.5[a] 15.6[b]	6.0 1.0	$4.\times10^{-13}$ $3.\times10^{-12}$	48. 4.1	5.5×10^{-14} 6.4×10^{-13}
$(B,v'=6)$	8.7 7.9	$1.\times10^{-5}$ $3.\times10^{-6}$	$3.\times10^{-7}$ $9.\times10^{-7}$	2.0×10^{-4} 6.6×10^{-5}	1.3×10^{-8} 4.0×10^{-8}
$(B,v'=9)$	7.8 6.8	$2.\times10^{-6}$ $4.\times10^{-7}$	$1.\times10^{-6}$ $7.\times10^{-6}$	1.3×10^{-4} 4.3×10^{-5}	2.0×10^{-8} 6.1×10^{-8}
$(B,v'=12)$	6.4 5.2	$2.\times10^{-7}$ $3.\times10^{-8}$	$1.\times10^{-5}$ $9.\times10^{-5}$	9.8×10^{-5} 3.2×10^{-5}	2.7×10^{-8} 8.1×10^{-8}
$(B,v'=15)$	5.0 3.3	$2.\times10^{-8}$ $1.\times10^{-9}$	$1.\times10^{-4}$ $3.\times10^{-3}$	7.9×10^{-5} 2.6×10^{-5}	3.4×10^{-8} 1.0×10^{-7}

[a] Upper values computed from the following $Ne\text{-}Cl_2$ potential parameters: $D_{Ne-Cl_2} = 55\ cm^{-1}$, $\alpha = 1.3\ Å^{-1}$, $\omega_{Cl_2}(X) = 560\ cm^{-1}$, $\omega_{Cl_2}(B) = 260\ cm^{-1}$.

[b] Lower values computed from:
$D_{Ne-Cl_2} = 80\ cm^{-1}$, $\alpha = 1.3\ Å^{-1}$, $\omega_{Cl_2}(X) = 560\ cm^{-1}$, $\omega_{Cl_2}(B) = 260\ cm^{-1}$.

predissociation lifetimes for the Ne-Cl_2 molecule. Two sets of potential parameters were used to estimate the lifetime:

a) D_{Ne-Cl_2} = 55 cm^{-1}, α = 1.3A^{-1}, $\omega_{Cl_2(X)}$ = 560 cm^{-1}, and $\omega_{Cl_2(B)}$ = 260 cm^{-1}.

b) D_{Ne-Cl_2} = 80 cm^{-1}, α = 1.3A^{-1}, $\omega_{Cl_2(X)}$ = 560 cm^{-1}, and $\omega_{Cl_2(B)}$ = 260 cm^{-1}.

These particular parameters were chosen so that the estimated bond dissociation energies should bracket the actual value. The Morse range parameter was chosen to be 1.3 $Å,^{-1}$ a bit smaller than the experimental value of 1.4 $Å^{-1}$ for Ne-I_2. Included in Table II are lifetimes of various states obtained from the "momentum-gap" correlation diagram. The "energy-gap" lifetime estimates were made by using the collinear rate calculated by the analytical formula derived from the harmonic approximation of the diatomic bond. It should be noted that order of magnitude increase in rate by considering the anharmonicity of the diatomic is approximately offset by the order of magnitude decrease in rate encountered by considering the perpendicular predissociation process. Both models predict a very long-lived Ne-$Cl_2(X,v''=1)$ complex and comparatively long-lived Ne-Cl_2 (B,v') species.

The lifetime estimates in Table II indicate that the lifetime broadening of the spectral lines of the Ne-Cl_2 molecule may be sufficiently small to permit resolution of individual rovibronic lines. Such measurements can potentially yield very accurate structural and lifetime information. Figure 10 illustrates the extent of rotational structure in the band computed for the best fit structure of Ne-Cl_2 with an effective linewidth of 100 MHz. Since the location of the bands for the complex have been determined, the high-resolution spectrum should be readily obtained with appropriate signal averaging. Further studies include searching for bands corresponding to vibrational progessions in the van

Figure 10. Lower trace is the calculated spectrum for the $Ne\text{-}Cl_2$ bandhead region at 100 MHz resolution. The bracket in the upper trace indicates the range of the high-resolution spectrum.

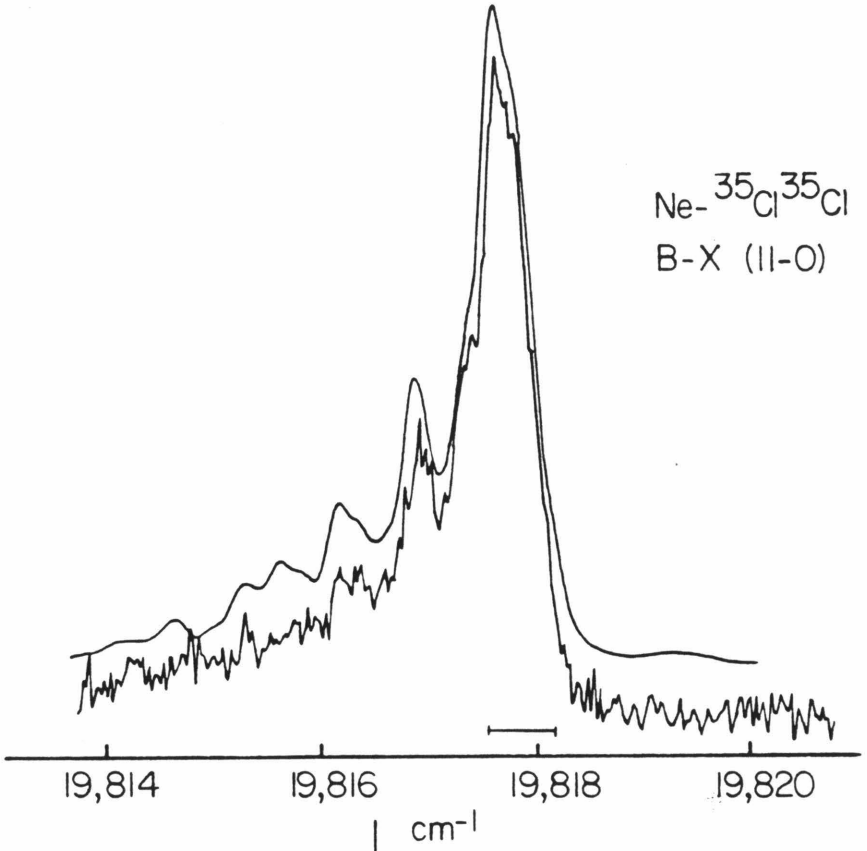
Ne-35Cl35Cl
B-X (11-0)
19,814
19,816
19,818
19,820
cm-1

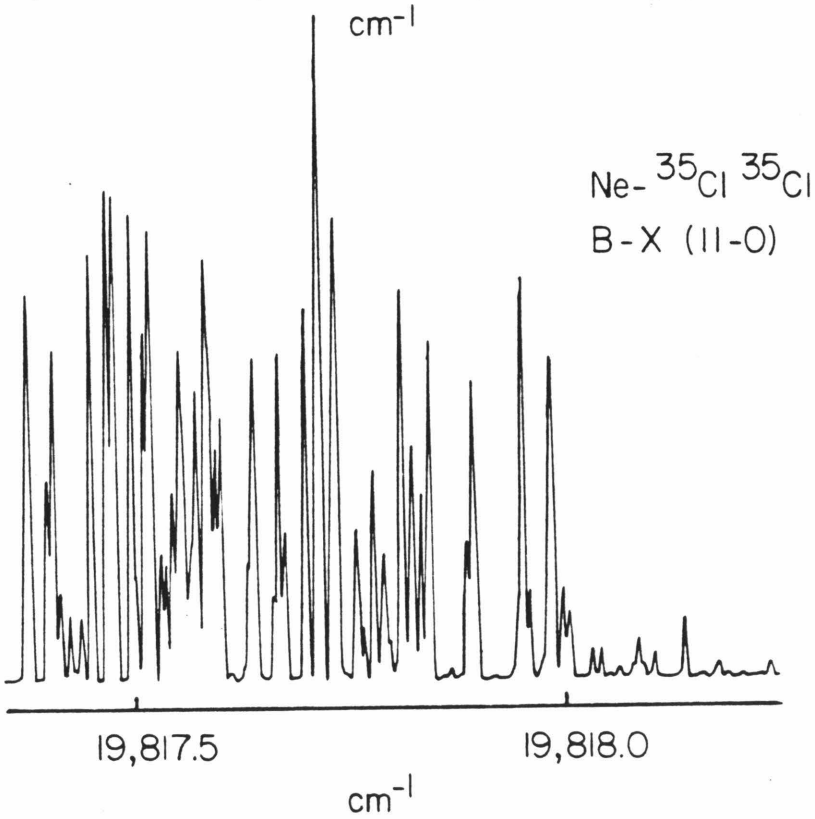
Ne-35Cl 35Cl
B-X (11-0)
19,817.5
19,818.0
cm-1

der Waals modes, and attempts to directly measure the lifetime of Ne-Cl_2 (X,v''=1). These studies will provide greater knowledge of the Ne-Cl_2 intermolecular potential and lifetime data to quantitatively test the accuracy of vibrational predissociation theoretical models.

In summary, the van der Waals molecule Ne-Cl_2 has been investigated by laser molecular beam spectroscopy. The molecule appears to be T-shaped with a Ne to Cl_2 center of mass distance of ~3.6 Å. The band shift data indicate that there may be some interaction with the repulsive limb of the bound $A^3\Pi_{1_u}$ state perturbing the Cl_2 $B^3\Pi_{(0_u^+)}$ state. The metastable vibrationally excited molecule Ne-Cl_2 (X, v''=1) was determined to have a lifetime of $>10^{-5}$ seconds. The Ne-Cl_2 molecule may be the first triatomic van der Waals complex to yield detailed intermoloecular potential data and precise lifetime information in its visible spectrum, providing an exacting test for theoretical vibrational predissociation models.

Acknowledgement

This work was supported by the National Science Foundation Grant No. CHE-8202408 and by the Atlantic Richfield Corporation. Acknowledgement is made to the Donors of the Petroleum Research Fund, administered by the American Chemical Society for partial support of this research.

V. References

1. R. E. Smalley, D. H. Levy, and L. Wharton, *J. Chem. Phys.* **64,** 3266 (1976).

2. R. E. Smalley, L. Wharton, and D. H. Levy, *J. Chem. Phys.* **68,** 671 (1978).

3. K. E. Johnson, L. Wharton, and D. H. Levy, *J. Chem. Phys.* **69,** 2719 (1978).

4. W. Sharfin, K. E. Johnson, L. Wharton, and D. H. Levy, *J. Chem. Phys.* **71,** 1292 (1979).

5. J. E. Kenny, K. E. Johnson, L. Wharton, and D. H. Levy, *J. Chem. Phys.* **72,** 1109 (1980).

6. K. E. Johnson, W. Sharfin, and D. H. Levy, *J. Chem. Phys.* **74,** 163 (1981).

7. J. A. Blazy, B. M. DeKoven, T. D. Russell, and D. H. Levy, *J. Chem. Phys.* **72,** 2439 (1980).

8. J. A. Beswick and J. Jortner, *Chem. Phys. Lett.* **49,** 13 (1977).

9. J. A. Beswick and J. Jortner, *J. Chem. Phys.* **68,** 2277 (1978).

10. J. A. Beswick and J. Jortner, *J. Chem. Phys.* **69,** 512 (1978).

11. J. A. Beswick, G. Delgado-Barrio, and J. Jortner, *J. Chem. Phys.* **70,** 3895 (1979).

12. J. A. Beswick and G. Delgado-Barrio, *J. Chem. Phys.* **73,** 3653 (1980).

13. G. E. Ewing, *Chem. Phys.* **29,** 253 (1978).

14. G. E. Ewing, *J. Chem. Phys.* **71,** 3143 (1979).

15. D. E. Brinza, B. A. Swartz, C. M. Western, and K. C. Janda, *J. Chem. Phys.* **79,** 1541 (1983).

16. Private communication with S. A. Rice and J. Tusa.

17. J. A. Coxon, *J. Quant. Spectrosc. Radiat. Transfer.* **11,** 1355 (1971).

18. J. A. Coxon, *J. Mol. Spectrosc.* **82,** 264 (1980).

19. M. P. Casassa, C. M. Western, F. G. Celii, D. E. Brinza, and K. C. Janda, *J. Chem. Phys.*, (in press).

20. J. M. Parsons, T. P. Schafer, F. P. Tully, P. E. Siska, Y. C. Wong, and Y. T. Lee, *J. Chem. Phys.* **53,** 2123 (1970).

21. M. A. A. Clyne and I. S. McDermid, *J. Chem. Soc., Faraday Trans. II.* **74,** 1935 (1978).

22. M. A. A. Clyne and I. S. McDermid, *J. Chem. Soc., Faraday Trans. II.* **75,** 1677 (1979).

23. S. J. Harris, S. E. Novick, W. Klemperer, and W. E. Falconer, *J. Chem. Phys.* **61,** 193 (1974).

24. D. Secrest and W. Eastes, *J. Chem. Phys.* **56,** 2502 (1972).

25. J. O. Hirschfelder, C. F. Curtiss, and R. B. Bird, *Molecular Theory of Gases and Liquids*, (Wiley, New York, 1954).